$$I_{ij} = m_j \times 10^{s_j x_i}$$

where mj and s_j re the geometrical mean value and the standard deviation for the j-th component, respectively.

Analysed values less than the detectable limit were treated as the half of the detectable limit shown Table II-2-7. Though 5 areas were studied, the statistical processing was carried out in one lump for all the areas.

The statistical processing was carried out except for the gabbroic rocks, because of these rocks show almost all under the detectable limit of PGM.

2-2-6 Evaluation of the Rock Geochemical Anomalies

1. Characteristics of univariate analysis

The geometrical mean values, logarithmic standard deviation, and other basic statistical values are shown in Table II-2-8. The frequency distributions of all the elements are shown in Appendex A-5.

Table II-2-8 Statistical parameter of rock geochemistry

	Au (ppb)	Ag (ppm)	Cu (ppm)	Co (ppm)	Ni (ppm)	Pt (ppb)	Pd (ppb)	Rh (ppb)	PGM (ppb)
No of smples	1,029	1,029	1,029	1,029	1,029	1,029	1,029	1,029	1,029
Geometric average	0.67	0.05	31.17	84.94	728.4	6.82	13.00	5.25	30.32
Minimum	0.50	0.01	2.00	0.50	11.00	5.00	5.00	5.00	15.00
Maximum	3,720	0.81	947	441	21,300	965	529	55	1,044
Standard deviation (logrithm)	0.38	0.55	0.64	0.18	0.28	0.37	0.56	0.12	0.43

The characteristics of the statistical values and frequency distributions of the univariate analysis for all over the area are as follows :

Gold: The geometrical mean value and the maximum value are 0.69 ppb and 3,720 ppb, respectively. The 83.9 % of the population are less than the detectable limit. The 16 % of the population are above the detectable limit. The relative frequency distribution of the Au shows that there are 2 populations whose maximum frequencies occurred at 5.62 ppb, and other populations whose frequencies are less than the detectable limit.

Silver: The geometrical mean value and the maximum value are 0.05 ppm and 9.81 ppm, respectively. The 12.2 % of the population are less than or the detectable limit. The relative frequency distribution of the Ag shows that there are 3 populations whose maximum frequencies occurred at 0.05 ppm shown large groupe, whose maximum frequencies occurred at 0.50 ppm shown small groupe of high grade, and other populations whose frequencies are less than the detectable limit.

Copper: The geometrical mean value and the maximum value are 31.2 ppm and 947 ppm, respectively. There is no population less than the detectable limit. The relative frequency distribution of the Cu shows that there are 2 populations whose maximum frequencies occurred at 7.9 ppm, and 200ppm, respectively.

Cobalt: The geometrical mean value and the maximum value are 84.9 ppm and 441 ppm, respectively. Only 2 samples are less than the detectable limit. The relative frequency distribution of the Co shows 1 population whose maximum frequencies occurred at 70.8 ppm, and with small fluctuation.

Nickel: The geometrical mean value, the maximum value, and the minimum value are 728 ppm, 21,300 ppm and 11 ppm, respectively. There is no value less than the detectable limit. The frequency distribution shows that there are a large population with the maximum frequency near 794 ppm and a small population with the peak frequency near 79 ppm.

Platinum: The geometrical mean value and the maximum value are 6.82 ppb and 965 ppb, respectively. The 84.9 % of the population are less than the detectable limit. The frequency distribution shows that there are large but low grade population less than the detectable limit and 2 high grade small population with the peak frequency near 20 ppb and 316ppb.

Palladium: The geometrical mean value and the maximum value are 13 ppb and 529 ppb, respectively. The 58.5 % of the population are less than the detectable limit. The frequency distribution shows that there are large but low grade population less than the detectable limit and 2 high grade small population with the peak frequency near 20 ppb and 79ppb.

Rhodium: The geometrical mean value and the maximum value are 5.3 ppb and 55 ppb, respectively. The 95.8 % of the population are less than the detectable limit. The frequency distribution shows that there are large but low grade population less than the detectable limit and 2 high grade small population with the peak frequency near 20 ppb and 28ppb. Only 43 samples are above the detectable limit. The characteristics of the whole populations are not clear.

PGM: The geometrical mean value and the maximum value are 30.32 ppb and 1,044 ppb, respectively. The 55.1 % of the population are less than the detectable limit. The frequency distribution shows that there are large but low grade population less than the detectable limit and 2 high grade small population with the peak frequency near 50 ppb and 126ppb.

Generaly, Gold and silver show low grade exept for one sample(Au 3,720ppb). copper has two different population and suggest to the existance of the mineralization. cobalt and nickel show one population with comparatively small fluctuation. PGM divided to large and low grade population less than the detectable limit and high grade small population.

2. Characteristics of the results of bivariate analysis

The correlation coefficients are shown in Table II-2-9. A scatter diagram and representative components are shown in Appendix A-6.

Table II-2-9 The matrix of the correlation coefficients

	Au	Ag	Cu	Co	Ni	Pt	Pb	Rh
Au	1.							
Ag	0.12	1.						
Cu	0.33	0.28	1.					
Co	0.03	-0.05	-0.26	1.				
Ni	0.04	-0.12	-0.34	0.70	1.			
Pt	0.49	0.08	0.17	0.07	0.07	1.		
Pd	0.09	-0.11	-0.26	0.22	0.23	0.37	1.	
Rh	0.15	0.00	0.02	0.03	-0.01	0.40	0.24	1.

Characteristics of correlation coefficents each other elements are as follows.

(1)The combinations whose correlation coefficents are more than 0.3 are cobalt-nickel groupe and PGM groupe.

(2)The correlation coefficients of gold and copper, gold and platinum are 0.33, 0.49 respectively.

(3)The correlation coefficients between silver, copper groupe and cobalt, nickel, paradium groupe are negative.

(4)Silver has no correlation coefficient with other elements.

(5)PGM has correlation coefficient with gold, but has no correlation coefficient with other elements.

3. Characteristics of each area

Distribution of each elements were shown in Fig.II-2-8-1 to Fig.II-2-10-9.

(1) EN, ES area

Gold: Comparatively high concentration is recognized on the central part of the EN02 survey line, and ES01, 02, 03, 06 lines, however, the distribution is spotted. Concentration zone correspond to upper potion of the P1 layer.

Silver: It widely distribute with low grade, and does not show the charactaristic distribution.

Copper: High copper zone concentrate in northern part of the EN and ES area, and distribute from upper potion of the P1 layer to gabbroic rocks.

Cobalt: Comparatively high concentration is continuously recognized from the EN02 toEN06 andfrom ES01 to ES06 survey line, however, the high cocentration zone above the 1 σ does not occur, low grade

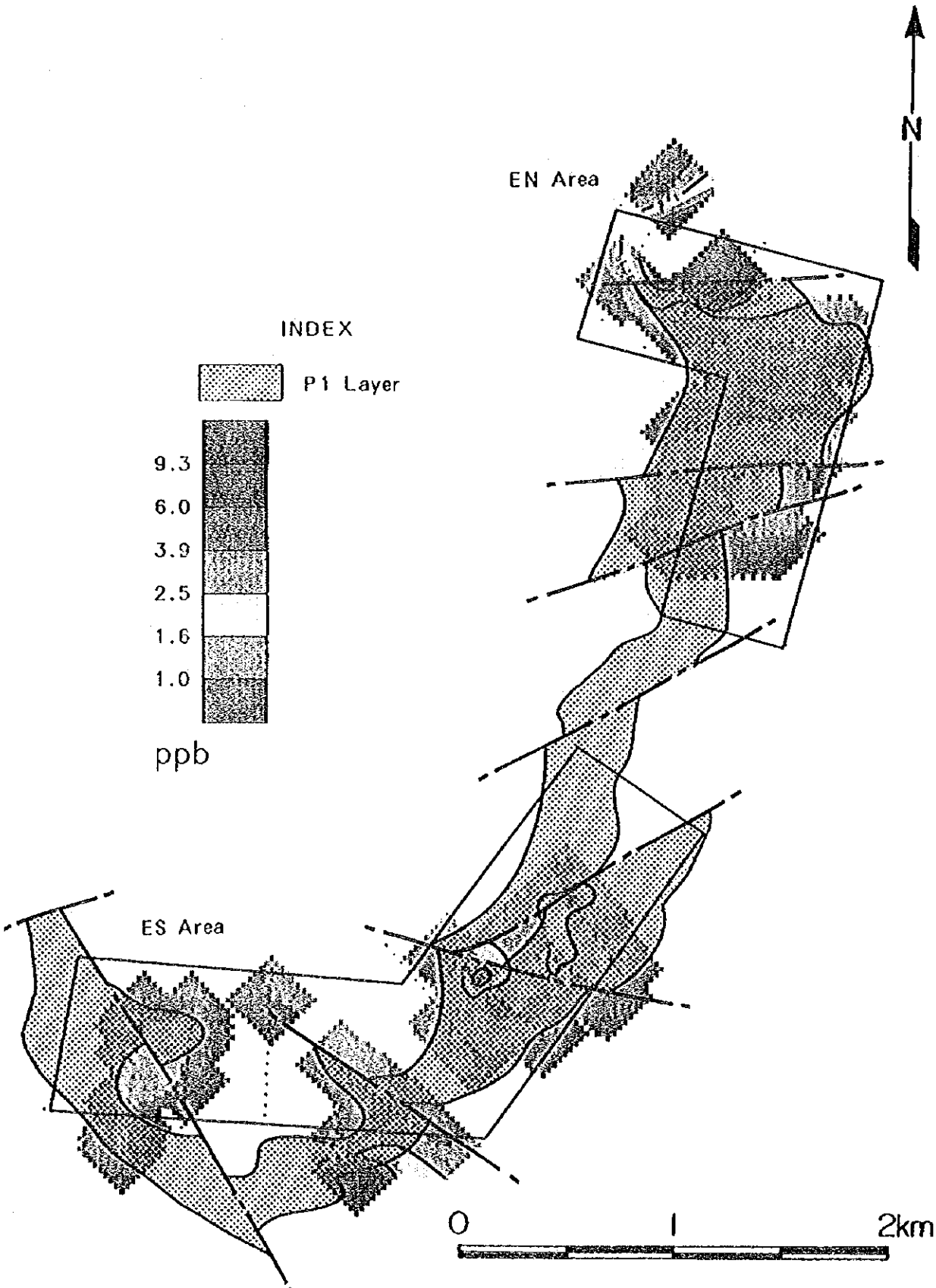

Fig.II-2-8-1 Distribution of Au content (EN, ES area)

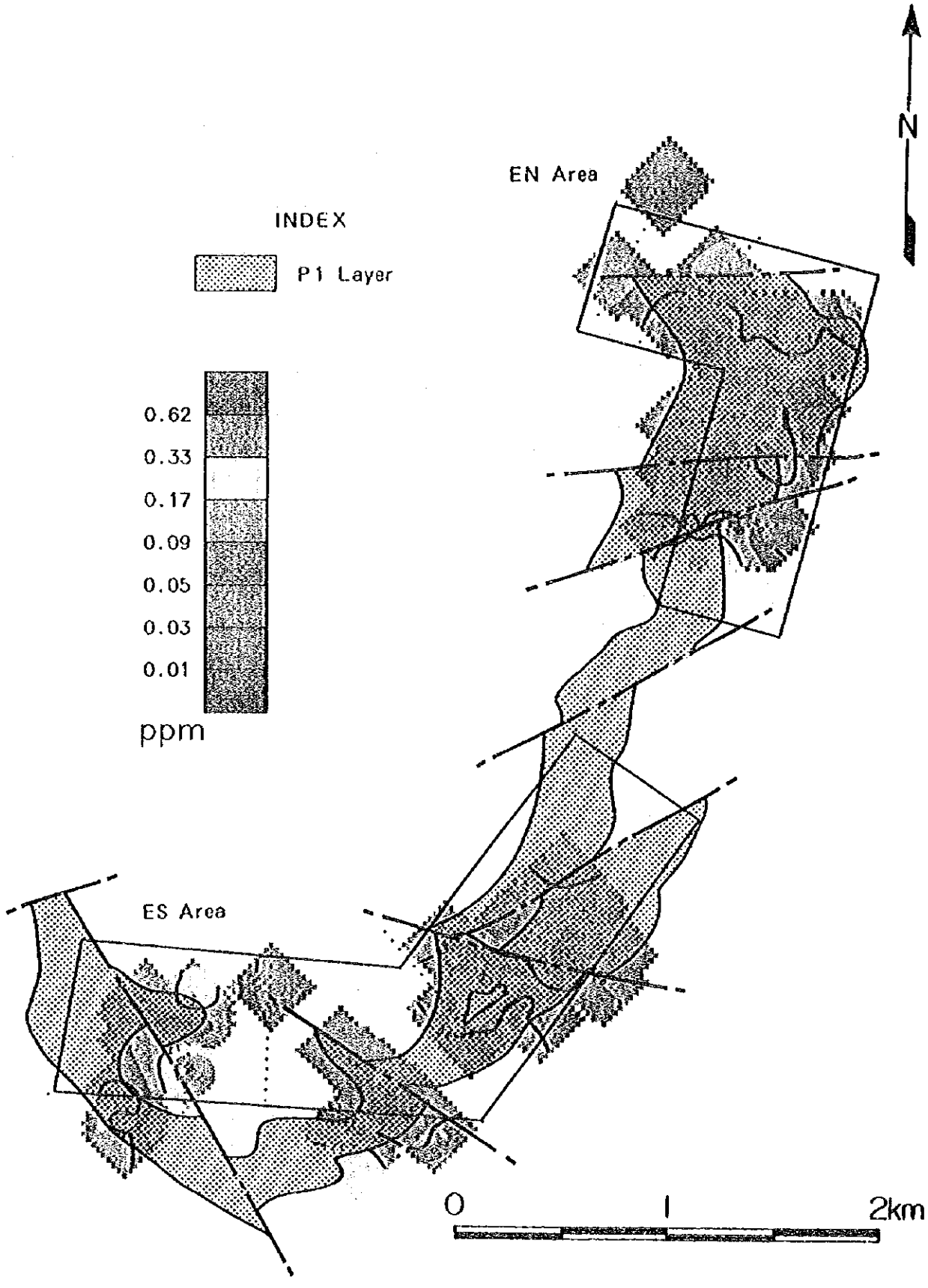

Fig.II-2-8-2 Distribution of Ag content (EN, ES area)

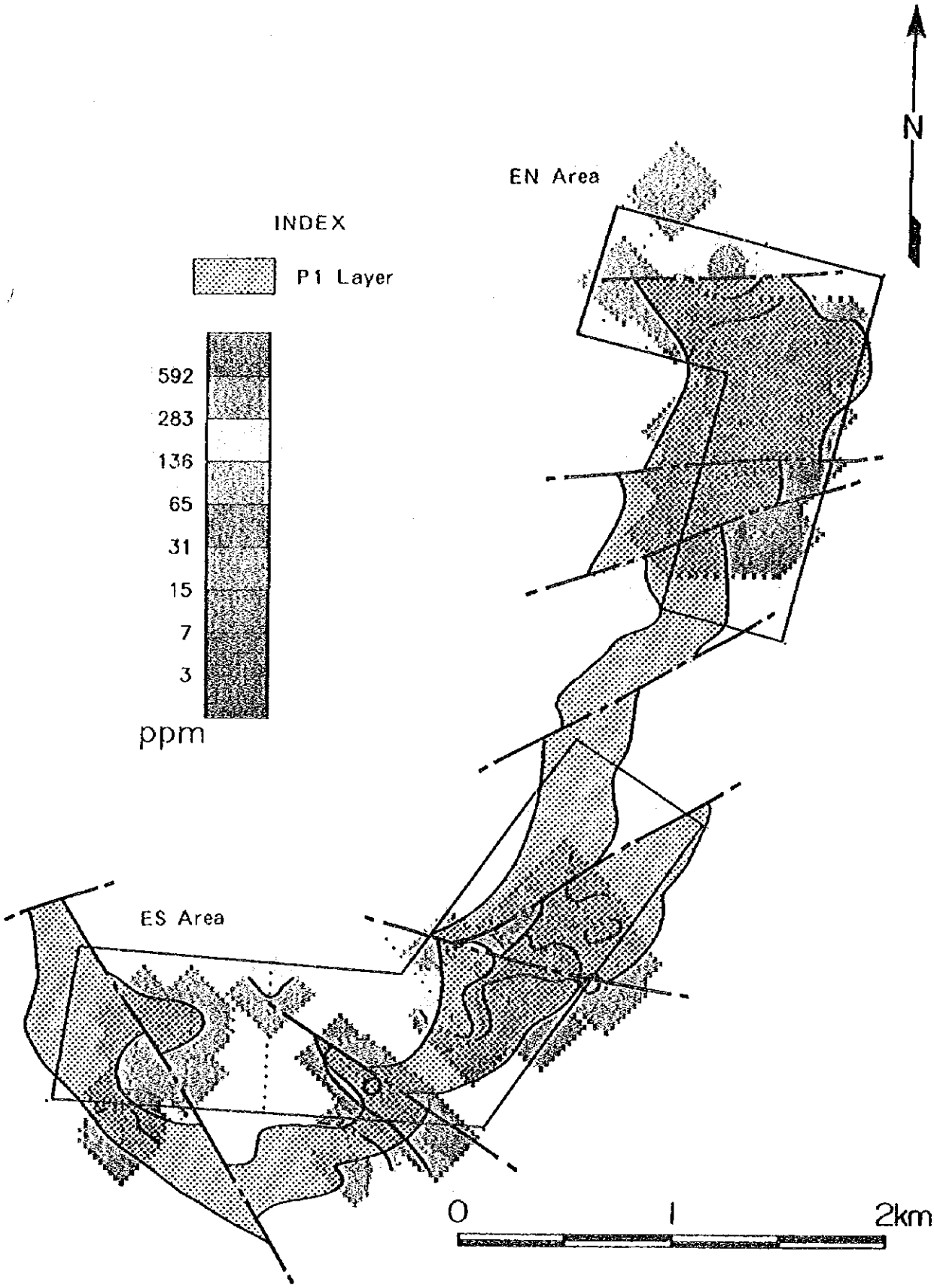

Fig.II-2-8-3 Distribution of Cu content (EN, ES area)

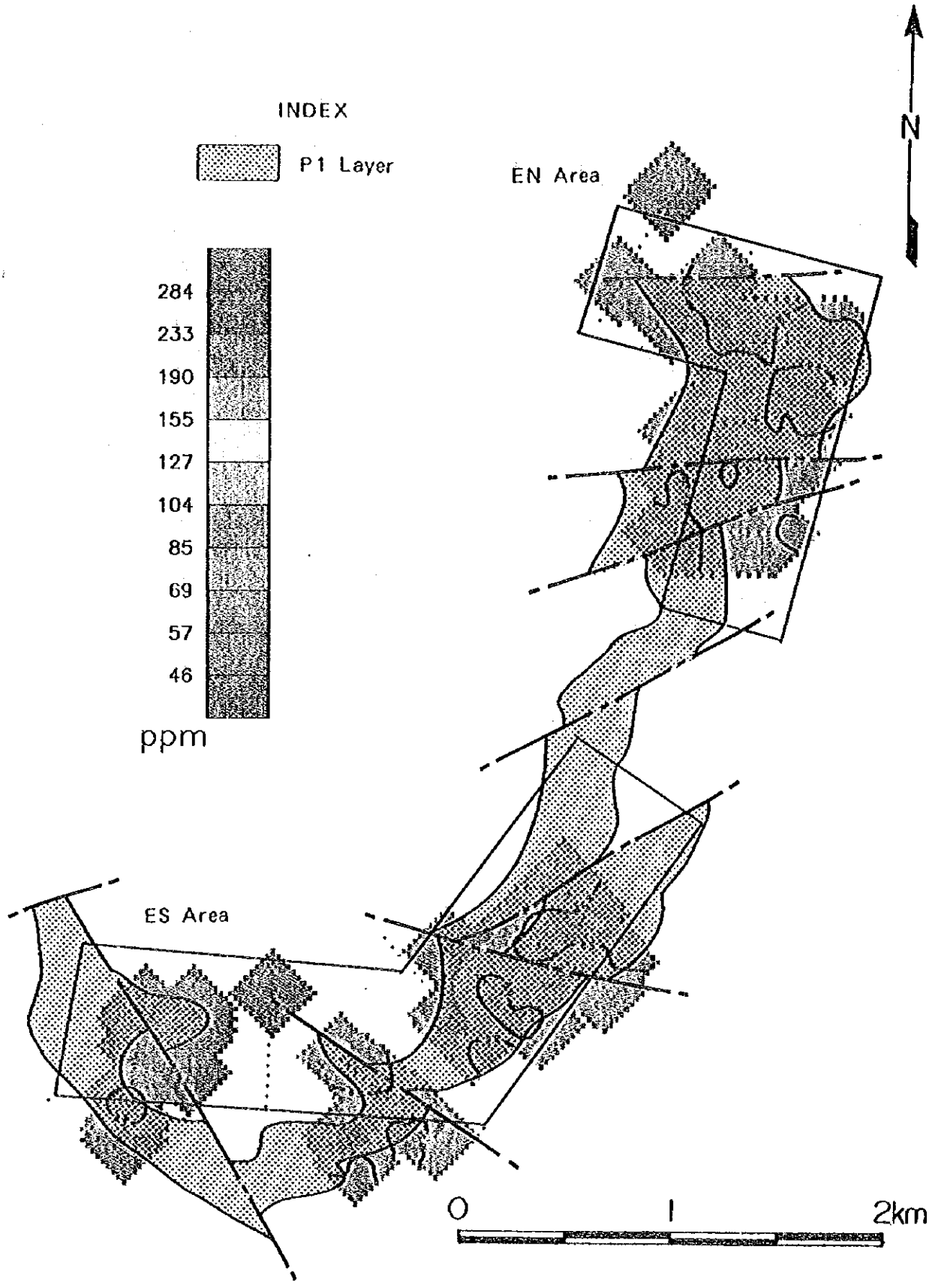

Fig.II-2-8-4 Distribution of Co content (EN, ES area)

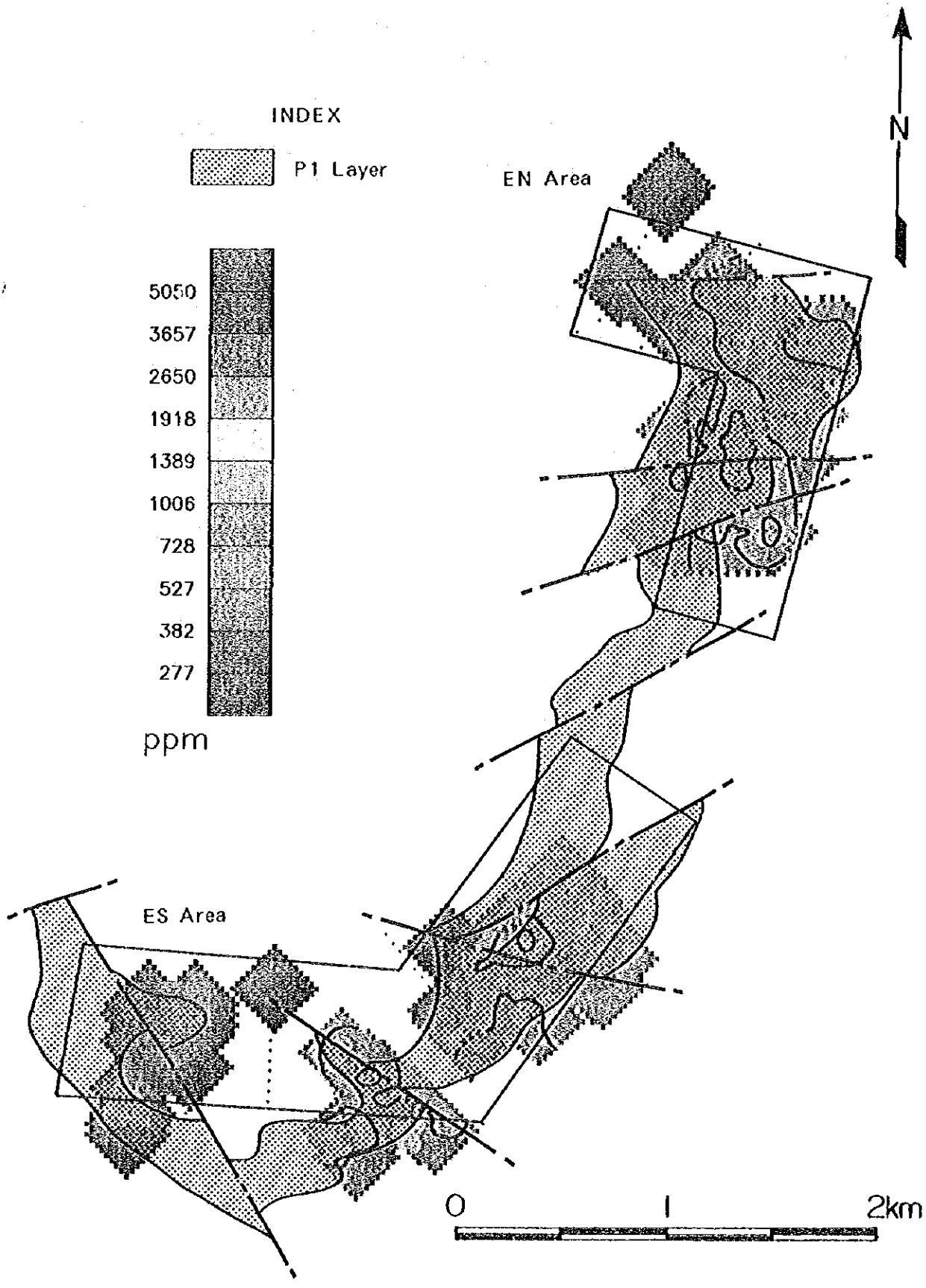

Fig.II-2-8-5 Distribution of Ni content (EN, ES area)

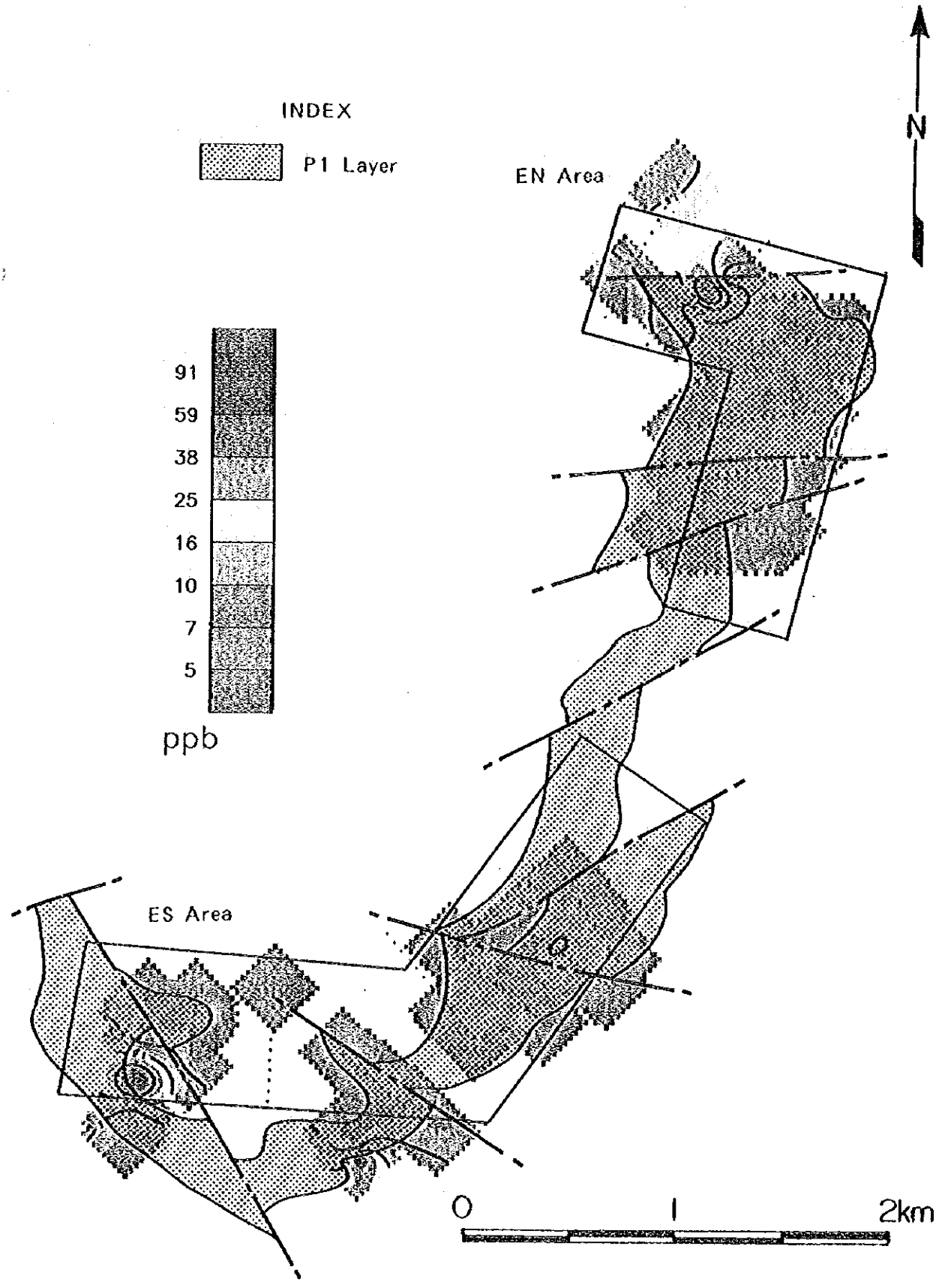

Fig.II-2-8-6 Distribution of Pt content (EN, ES area)

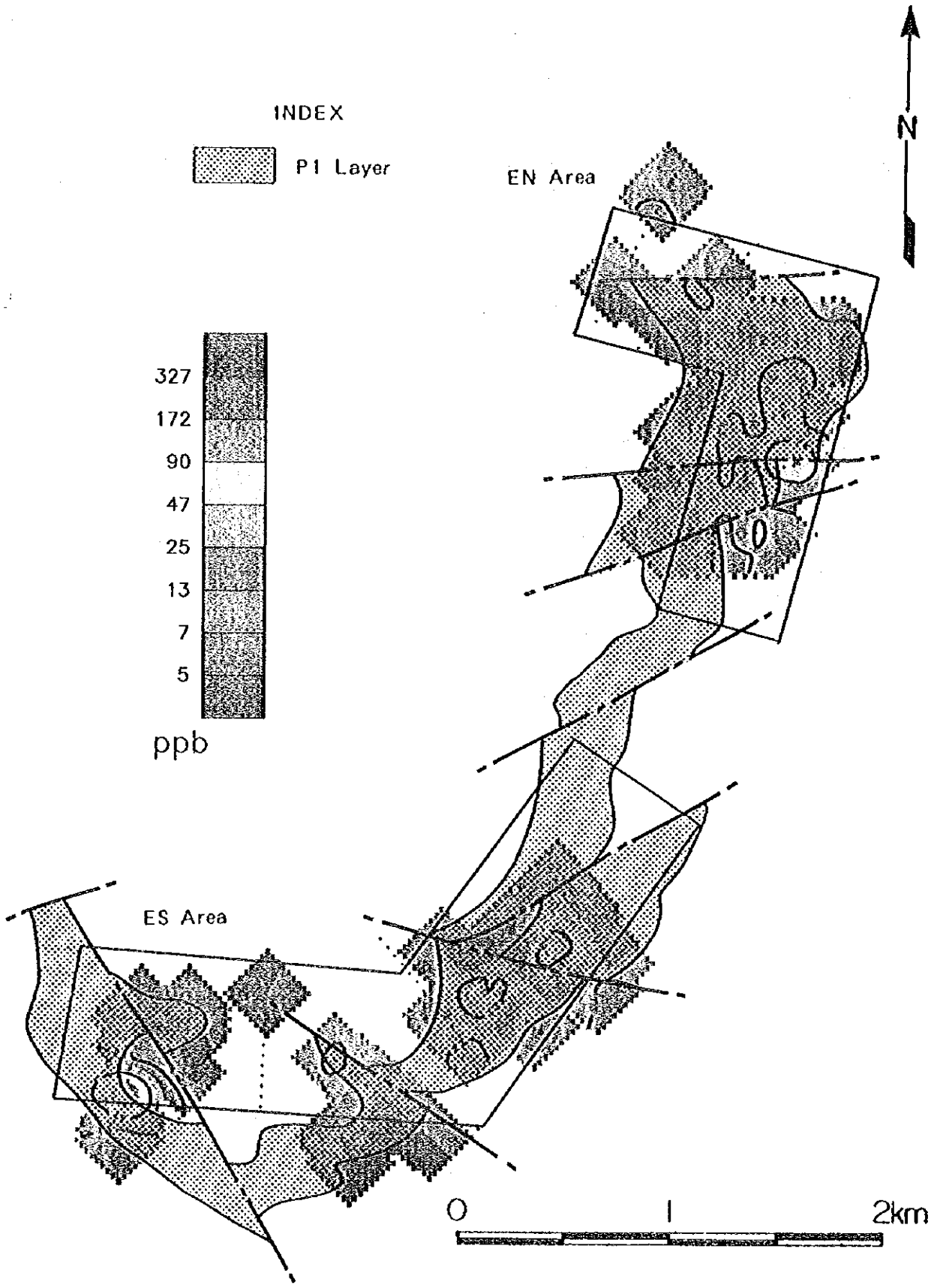

Fig.II-2-8-7 Distribution of Pd content (EN, ES area)

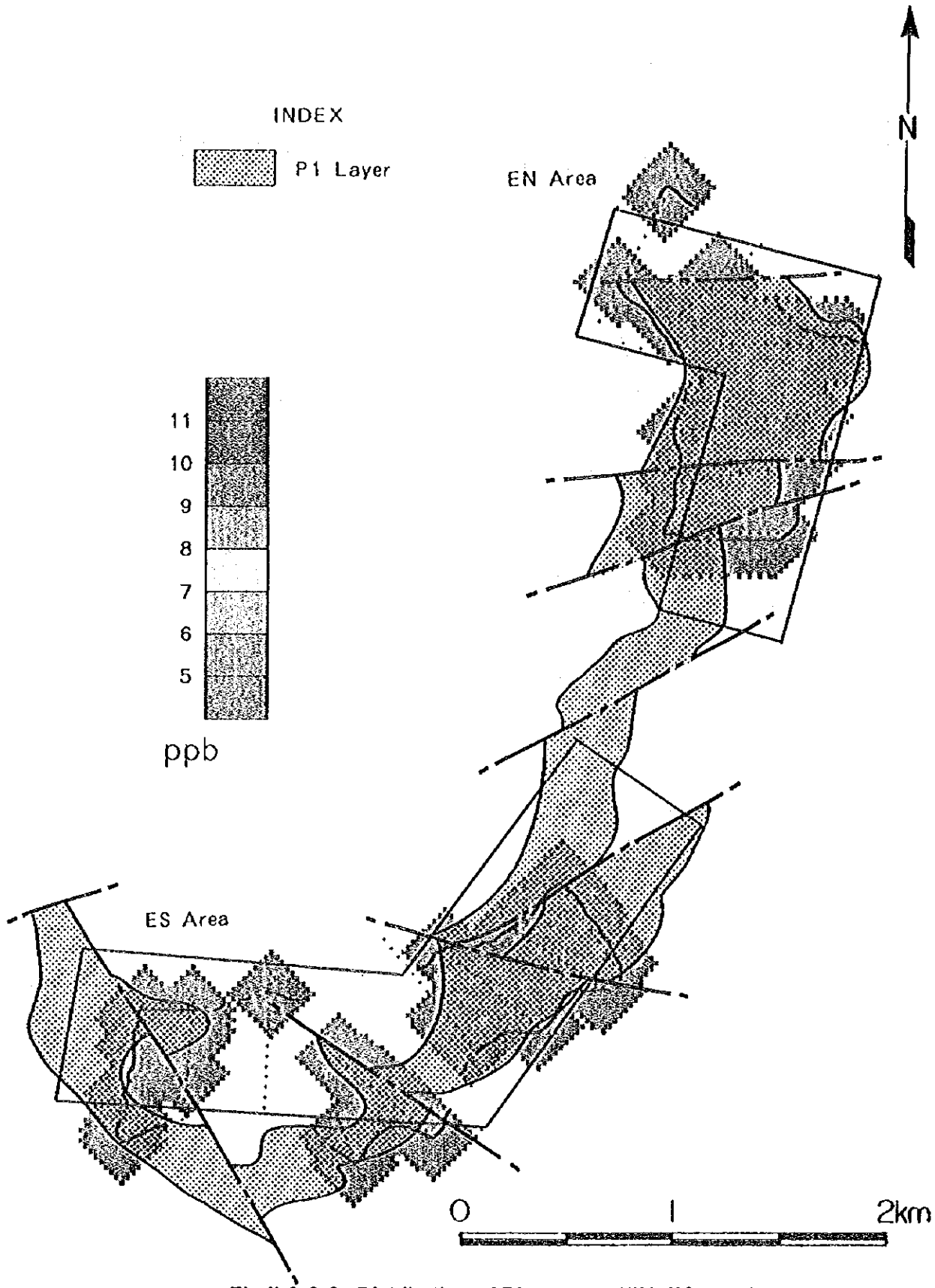

Fig.II-2-8-8 Distribution of Rh content (EN, ES area)

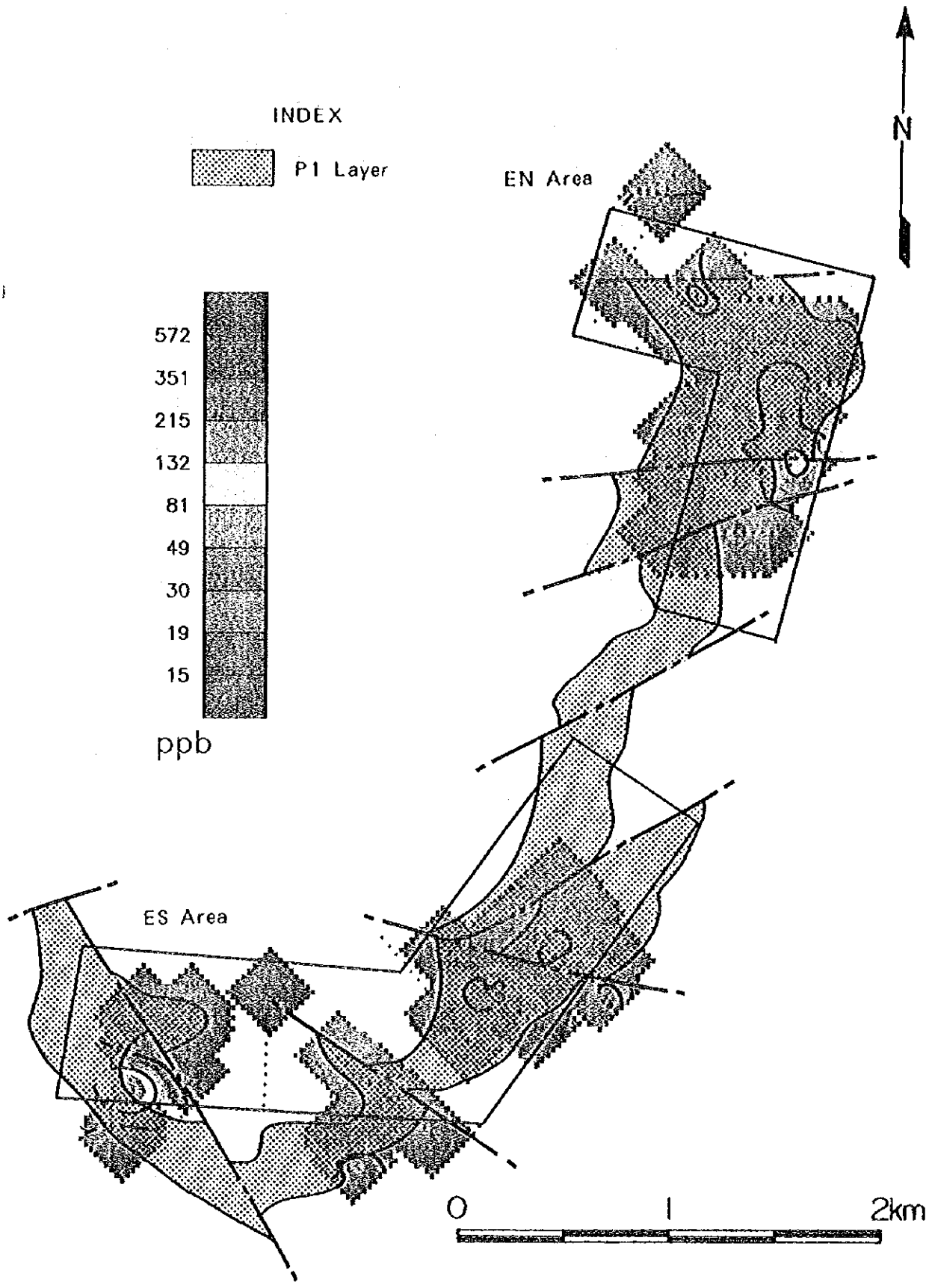

Fig.II-2-8-9 Distribution of PGM content (EN, ES area)

( )

( )

( )

zone widely distribute. Concentration zone correspond from lower potion of the P1 layer to lower serpentinite.

Nickel: Distribution form is similar to cobalt, high concentration zone clearly correspond to lower potion of the P1 layer.

Platinum: Comparatively high concentration is recognized on the EN02, ES02, 06, 09 lines, however, the distribution is spotted.There is no continuous distribution.

Palladium: Comparatively high concentration is recognized on the EN02, EN03～EN06, ES02～ES04 and ES09 lines, however, the distribution is spotted. Continuous distribution can not recognize, high concetrated points are not overlapped to pratinum, and correspond to lower potion of the P1 layer.

Rhodium: Analitical values are all less than the detectable limit.

PGM: Comparatively high concentration is recognized on the EN02, 04, 05, ES02, 03, 06, 09 lines, however, the distribution is spotted.There is no continuous distribution.

(2) CB area

Gold: Comparatively high concentration is continuously recognized on the CB03 to CB08 and CB17 to CB20 survey lines, the distribution become spotted between CB10 and CB13 lines. Concentration zone correspond to middle to lower potion of the P1 layer.

Silver: It widely distribute with low grade, thereis no corresponding with geological situation.

Copper: Wide and continuous high copper zone is recognized in east part of the CB02～CB08 lines and west part of the CB10～CB20 lines, and distribute from upper potion of the P1 layer to gabbroic rocks.

Cobalt: Comparatively high concentration is continuously recognized from the CB03 toCB12 survey line. Concentration zone correspond to lower potion of the P1 layer.

Nickel: Distribution form is similar to cobalt, high concentration zone clearly correspond to lower potion of the P1 layer.

Platinum: Comparatively high concentration is continuously recognized between CB04 to CB08 and CB17 to CB18 lines, the high cocentration zone above the 2 σ occur between CB04 and CB08 lines,correspond to upper potion of the P1 layer.

Palladium: Comparatively high concentration is continuously recognized between CB03 and CB18 lines,

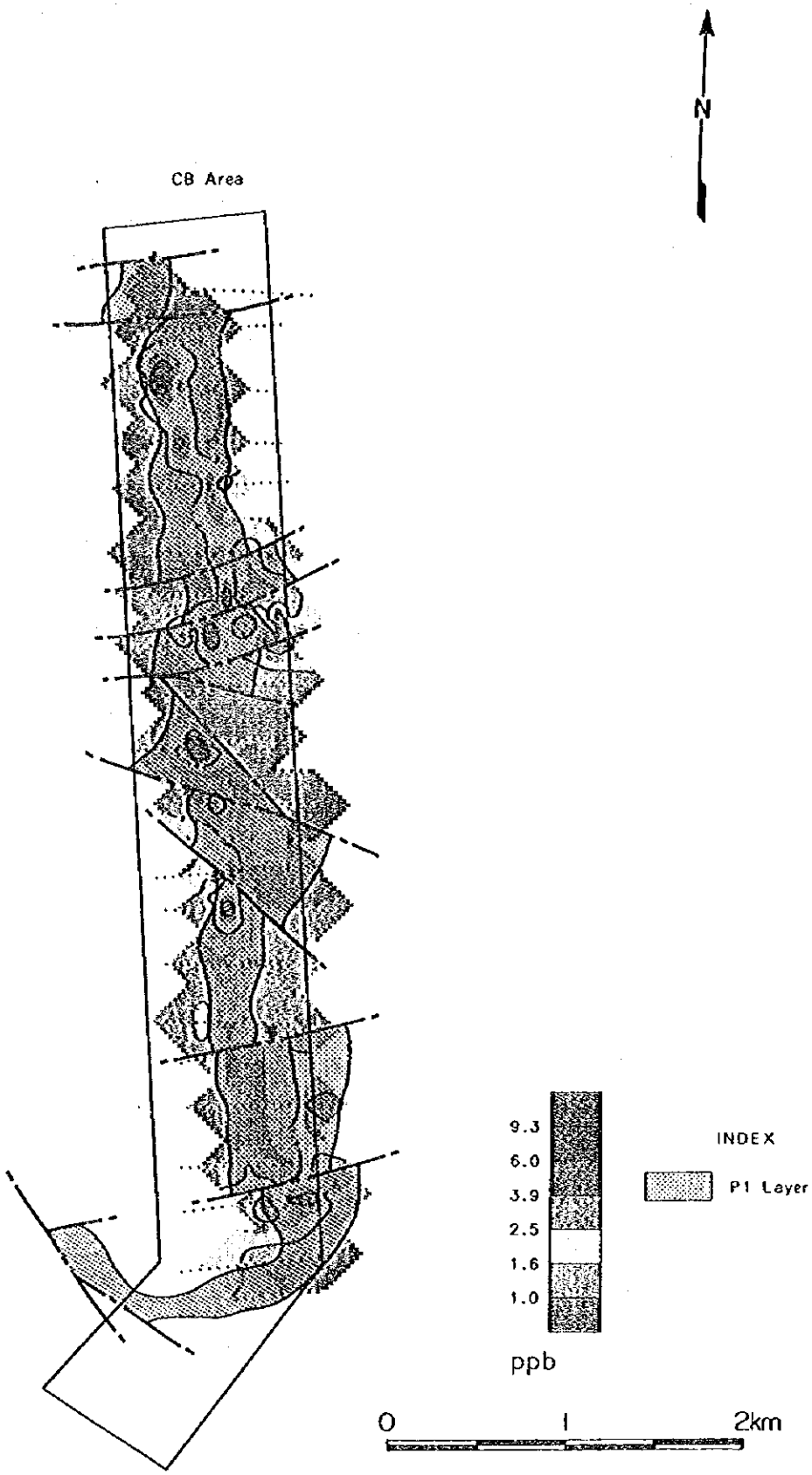

Fig.II-2-9-1 Distribution of Au content (CB area)

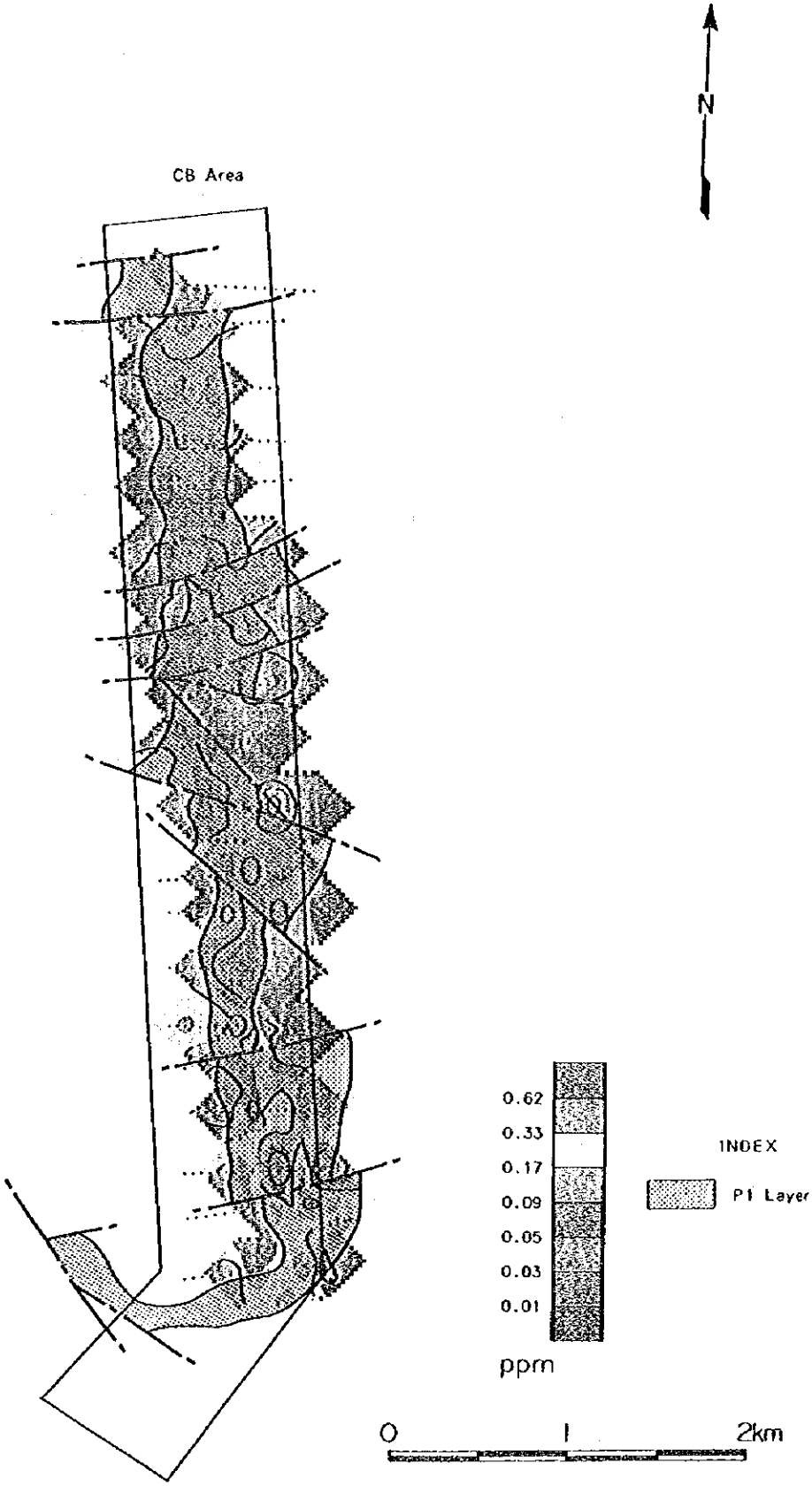

Fig.II-2-9-2 Distribution of Ag content (CB area)

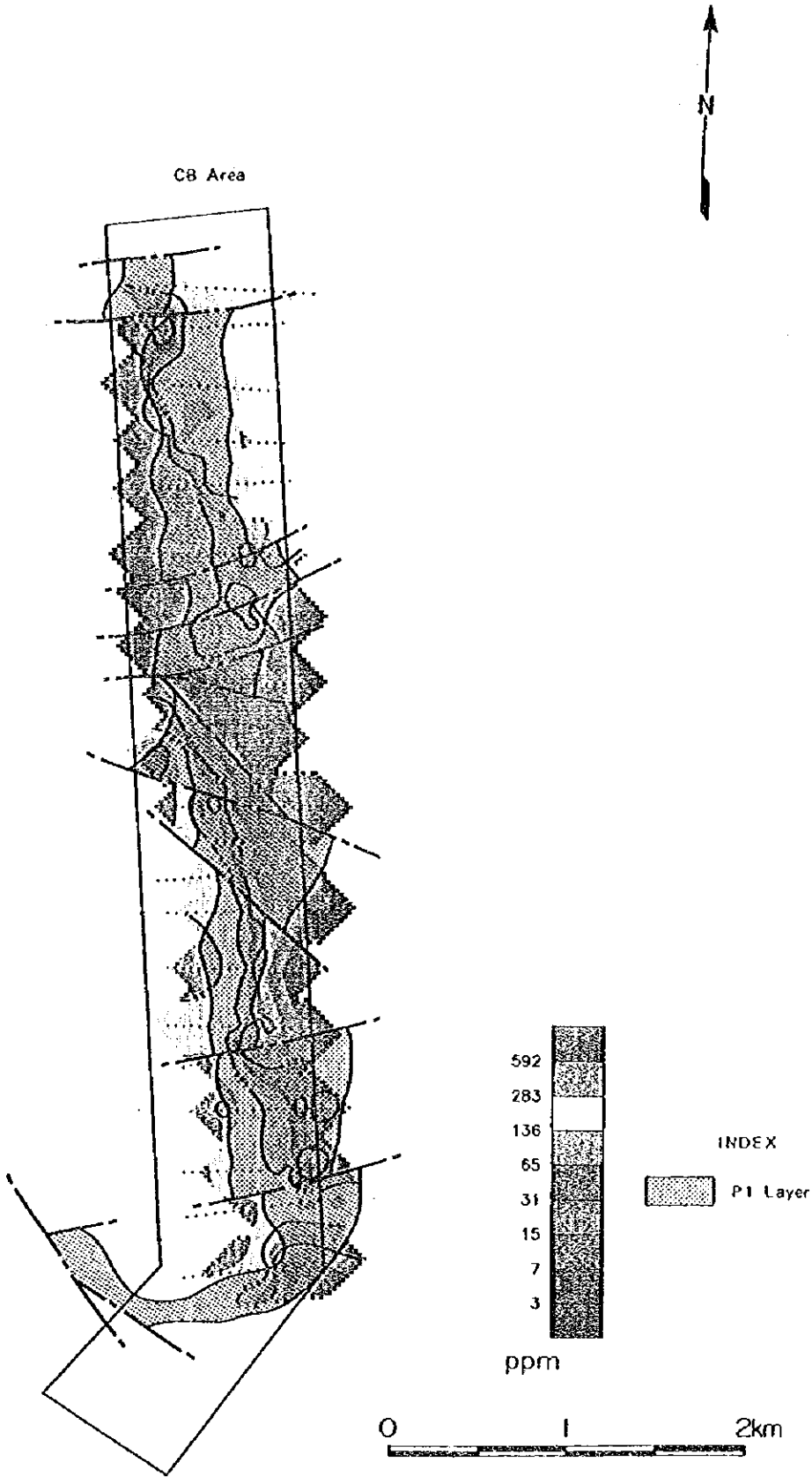

Fig.II-2-9-3 Distribution of Cu content (CB area)

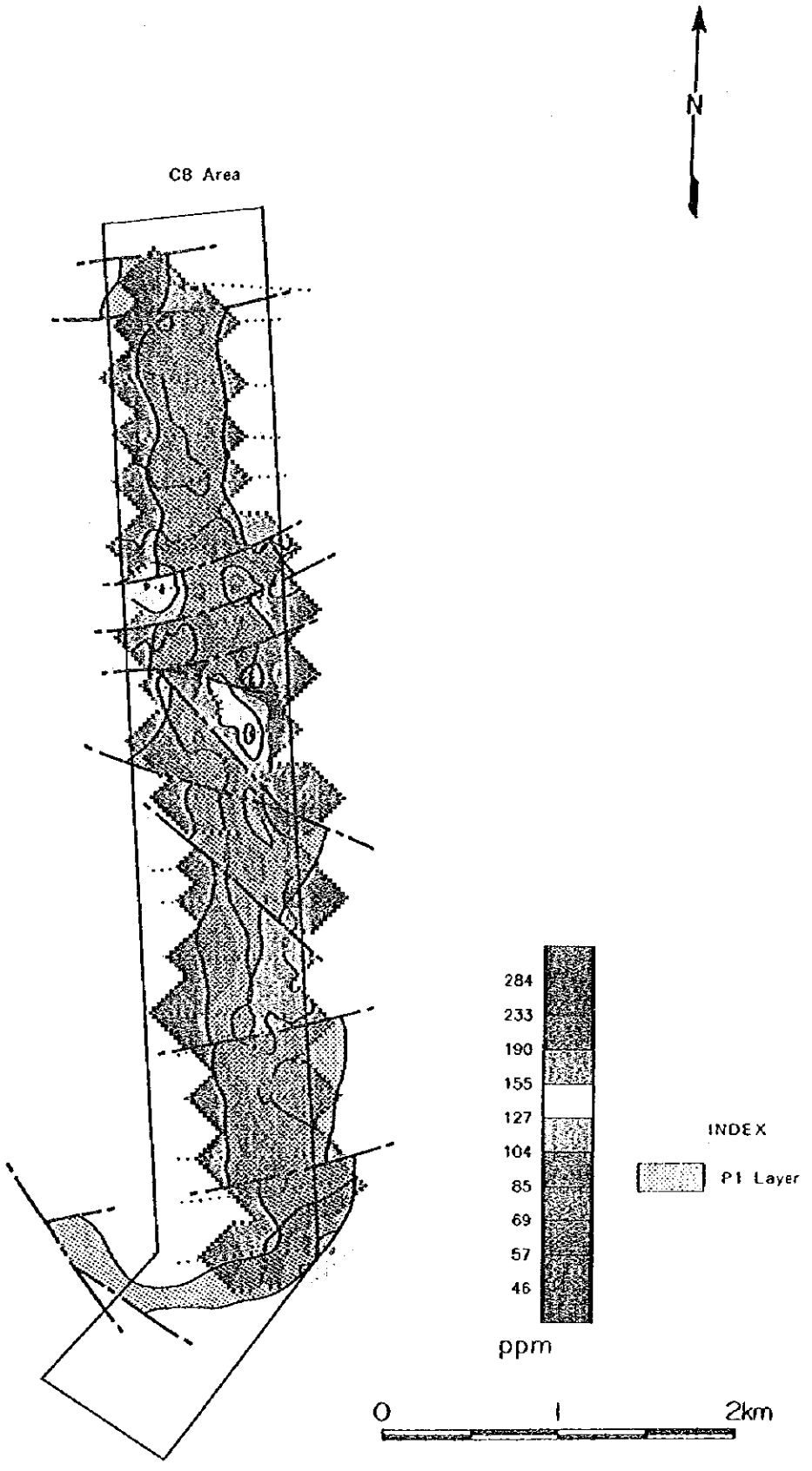

Fig.II-2-9-4 Distribution of Co content (CB area)

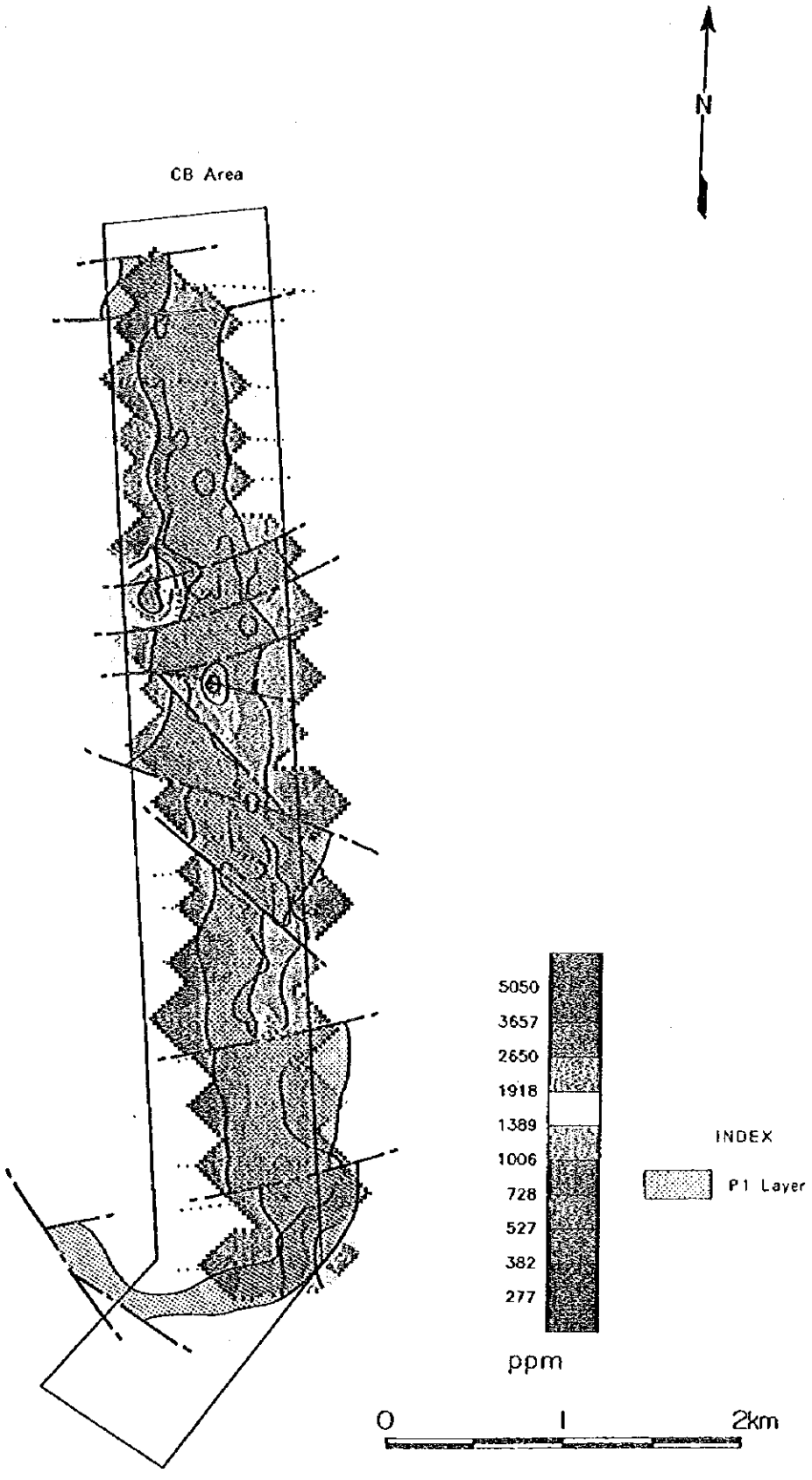

Fig.II-2-9-5 Distribution of Ni content (CB area)

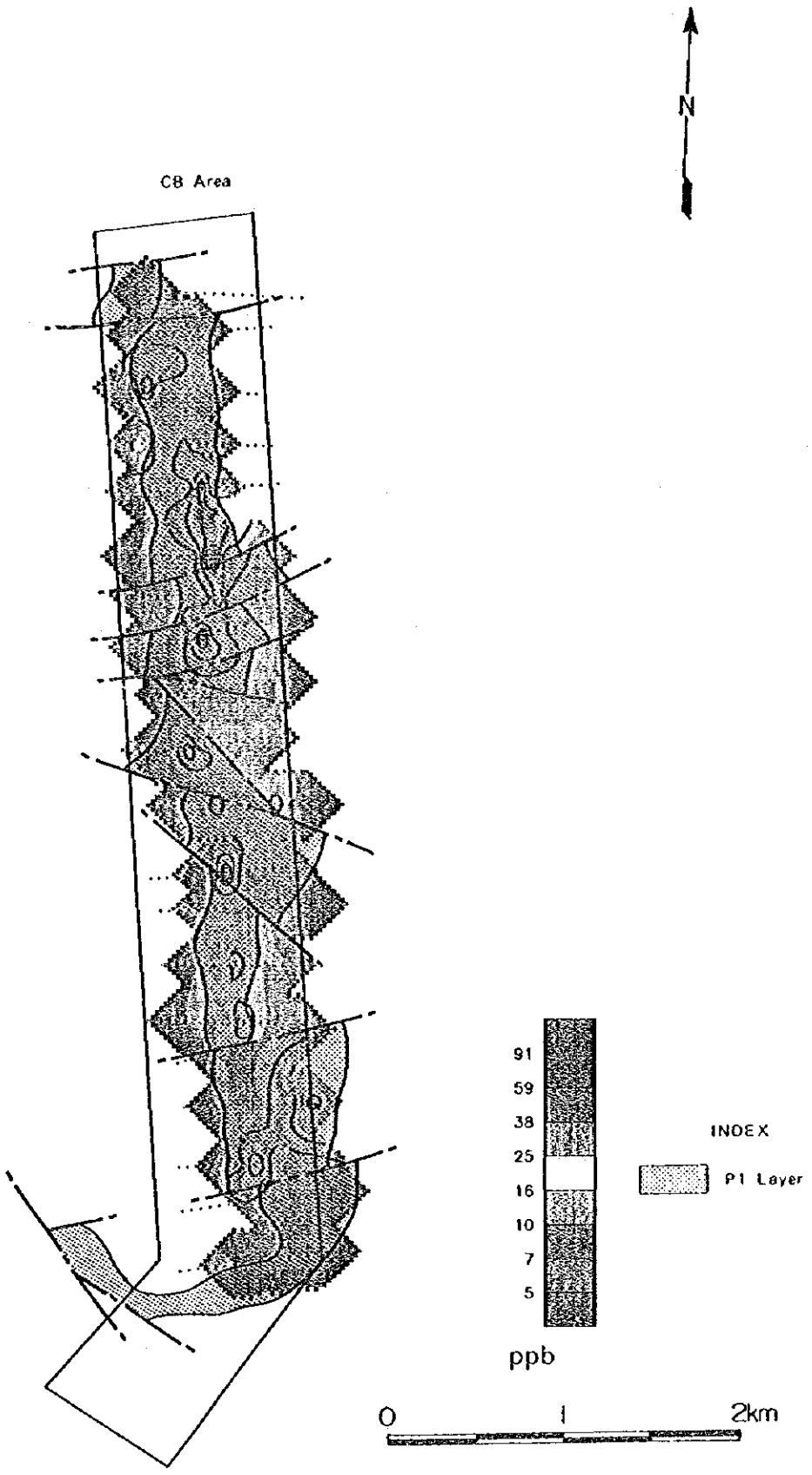

Fig.II-2-9-6 Distribution of Pt content (CB area)

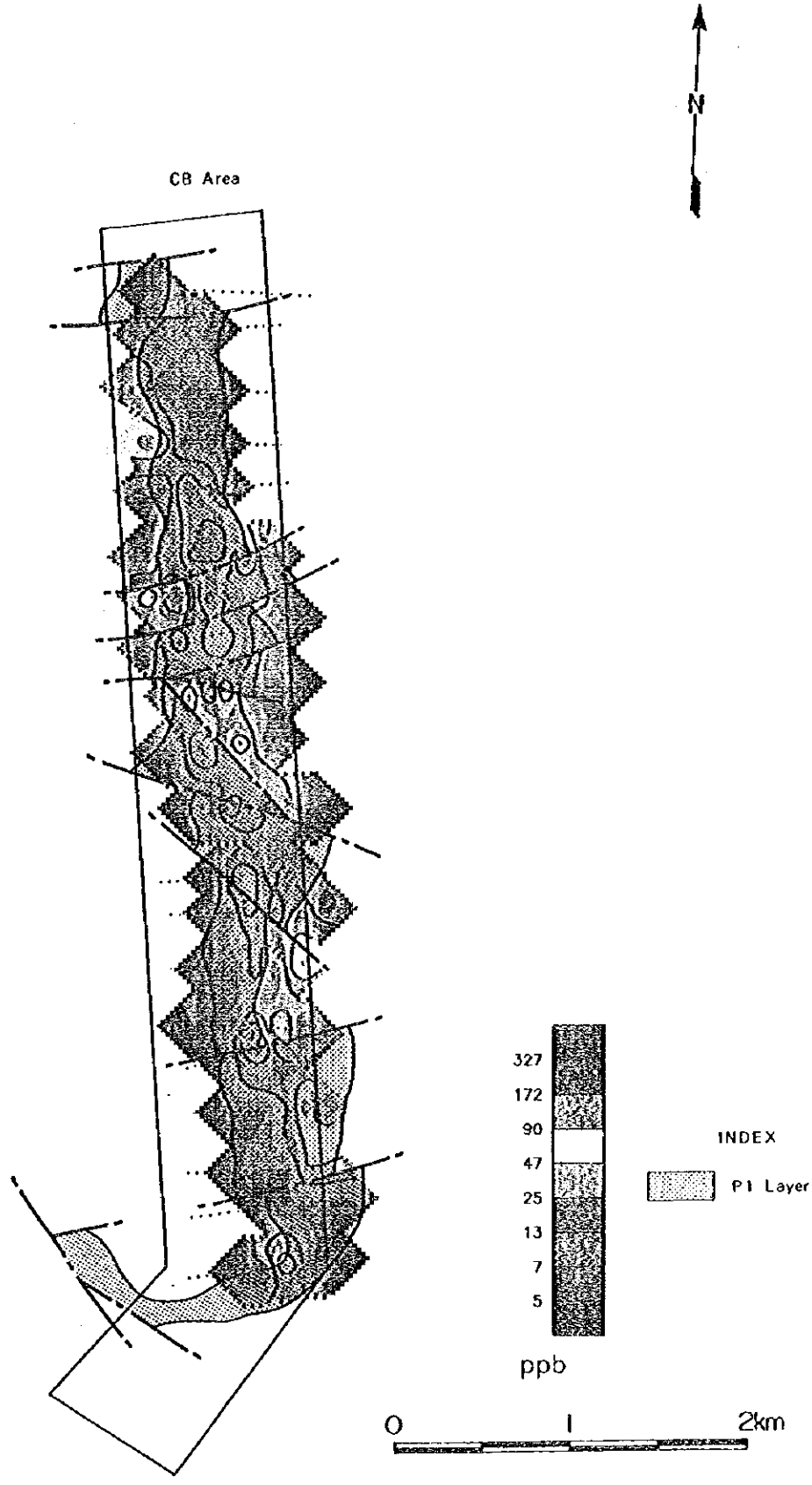

Fig.II-2-9-7 Distribution of Pd content (CB area)

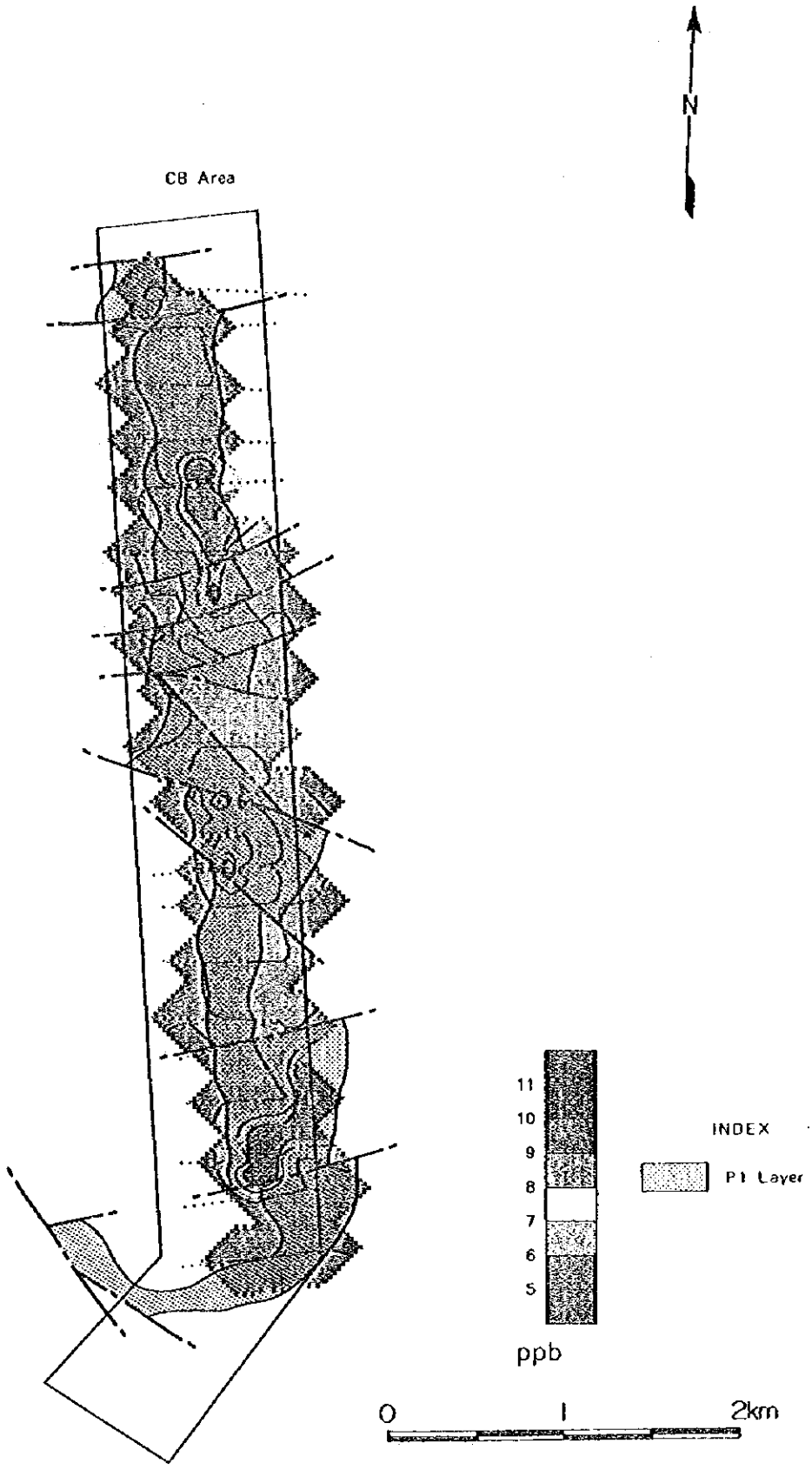

Fig.II-2-9-8 Distribution of Rh content (CB area)

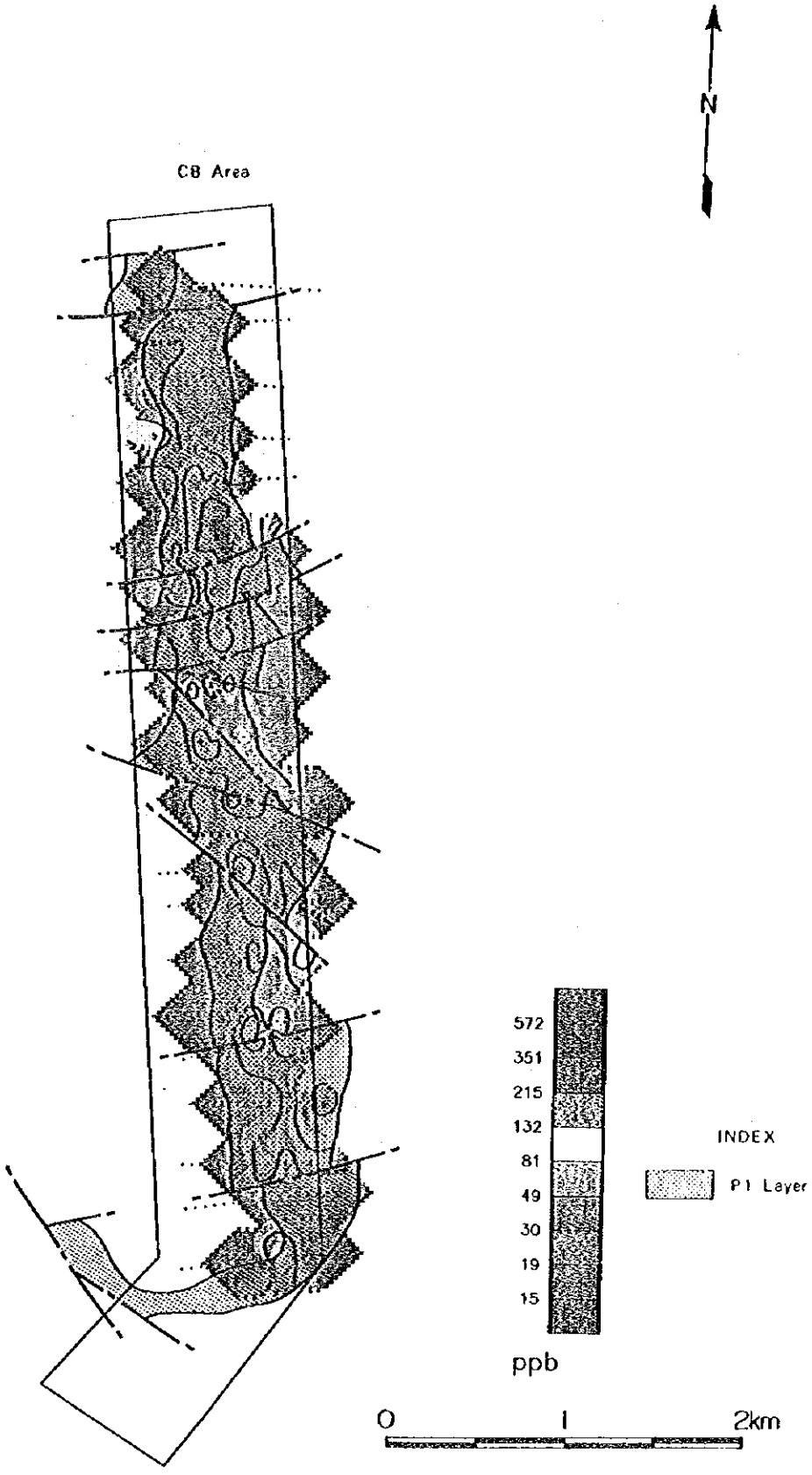

Fig.II-2-9-9 Distribution of PGM content (CB area)

( )

( )

( )

the high cocentration zone above the 1 σ ~ 2 σ occur between CB05 and CB08 lines, Pd distribution in this area is almost overlapped with Pt.

Rhodium: Rh distribution in this area is almost overlapped with Pt, Pd.

PGM: Comparatively high concentration iscontinuously recognized between CB03 and CB18 lines, the high cocentration zone above the 1 σ ~ 2 σ occur between CB05 and CB08 lines.

(3) WN, WS area

Gold: Comparatively high concentration is spotted, and Continuous distribution does not be recognized in the WN area. Narrow high concentrated distribution occur in the middle potion of the P1 layer with north to south derection in the WS area.

Silver: It widely distribute with low grade, there is no corresponding with geological situation.

Copper: Wide and continuous high copper zone recognized in southeastern part of the WN area and eastern half of the WS area, and distribute from upper potion of the P1 layer to gabbroic rocks. This copper high concentrated zone correspond to the distribution of the sulphide dissemination in the field.

Cobalt: Comparatively high concentration is continuously recognized through the WN and WS area. Concentration zone correspond to lower potion of the P1 layer. The high cocentration zone above the 1 σ occur in the lower serpentinite.

Nickel: Comparatively high concentration is continuously recognized in northeastern part of the WN area and western half of the WS area, The high cocentration zone above the 1 σ has a tendency to occur in the lower serpentinite.

Platinum: Comparatively high concentration is continuously recognized between WN012~WN13 and WS05~WS17ines, the high cocentration zone above the 1 σ ~2 σ is accompanied,correspond to middle potion of the P1 layer. High concentration is also recognized between WN014~WN23 but the zone is not continuous cutting by fault. the high cocentration zone partly occur in the lower serpentinite.

Palladium: Comparatively high concentration is continuously recognized between WN012~WN13 and WS01~WS17ines, the high cocentration zone above the 1 σ ~2 σ is accompanied,correspond to middle potion of the P1 layer. High concentration is also recognized between WN014~WN23 but the zone is not continuous cutting by fault. the high cocentration zone above the 1 σ partly occur in the lower serpentinite. The distribution is almost overlapped to Platinum.

Rhodium: Rh distribution in this area is almost overlapped with Pt, Pd but clear tendency is not recognized.

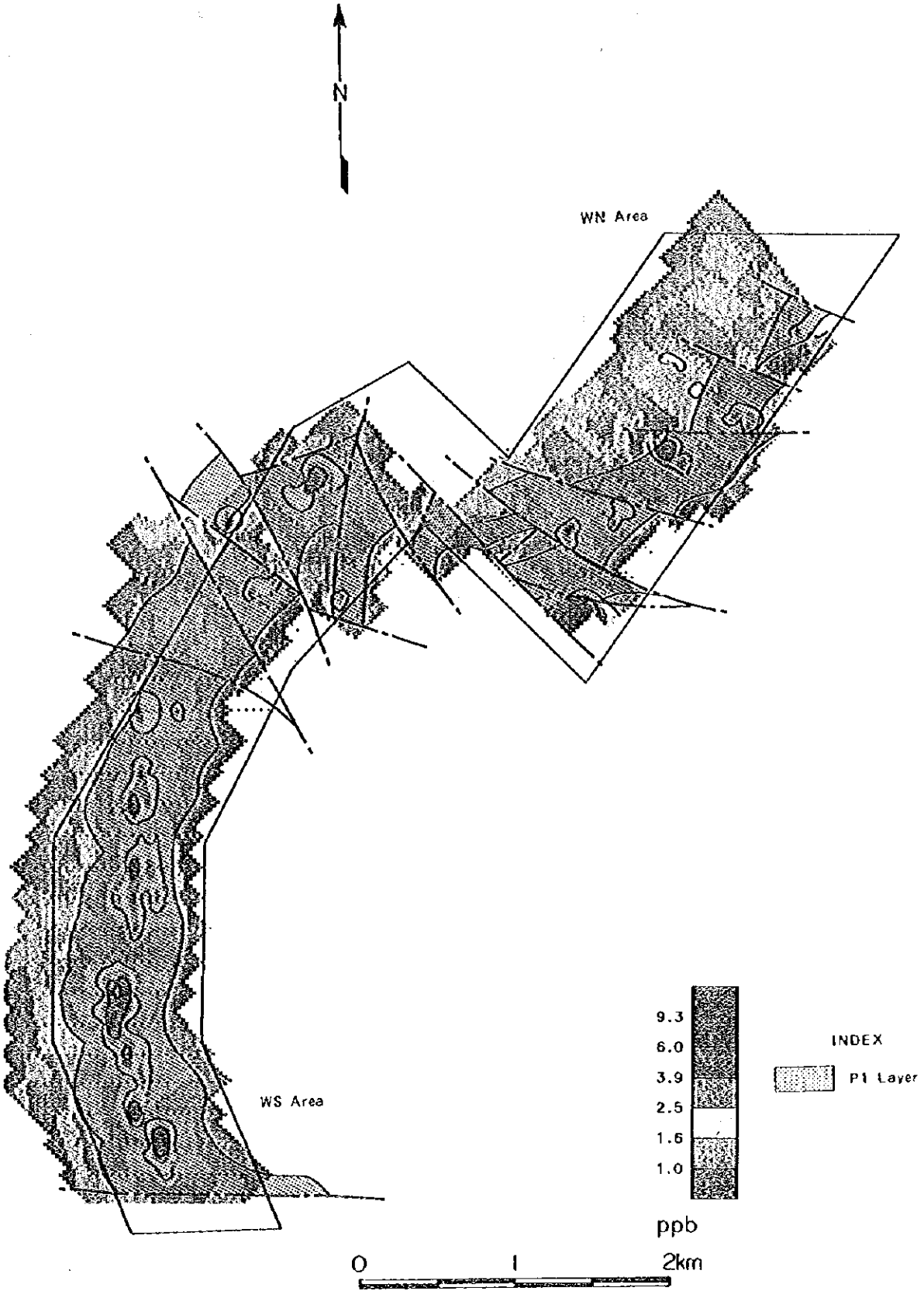

Fig.II-2-10-1 Distribution of Au content (WN, WS area)

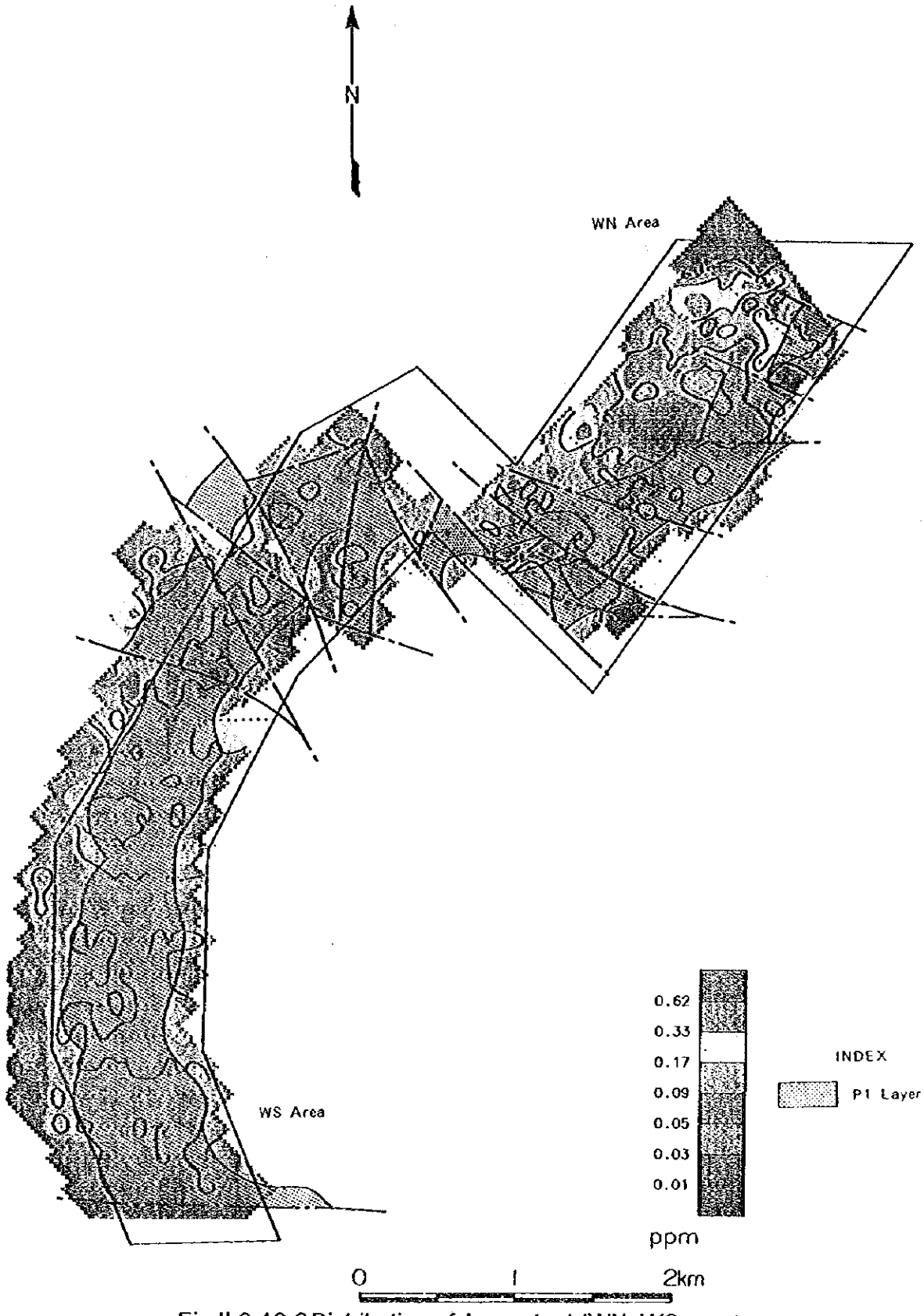

Fig.II-2-10-2 Distribution of Ag content (WN, WS area)

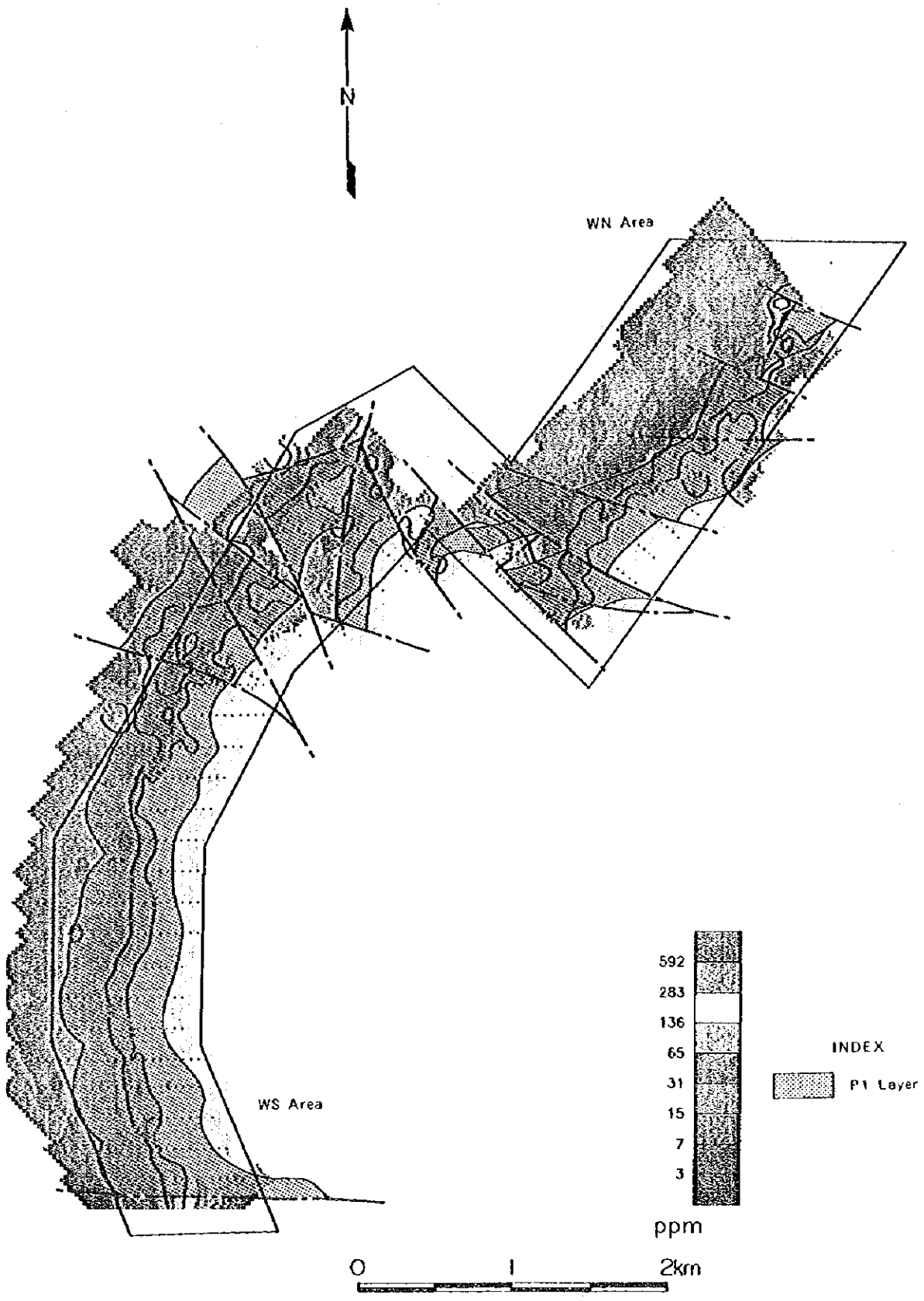

Fig.II-2-10-3 Distribution of Cu content (WN, WS area)

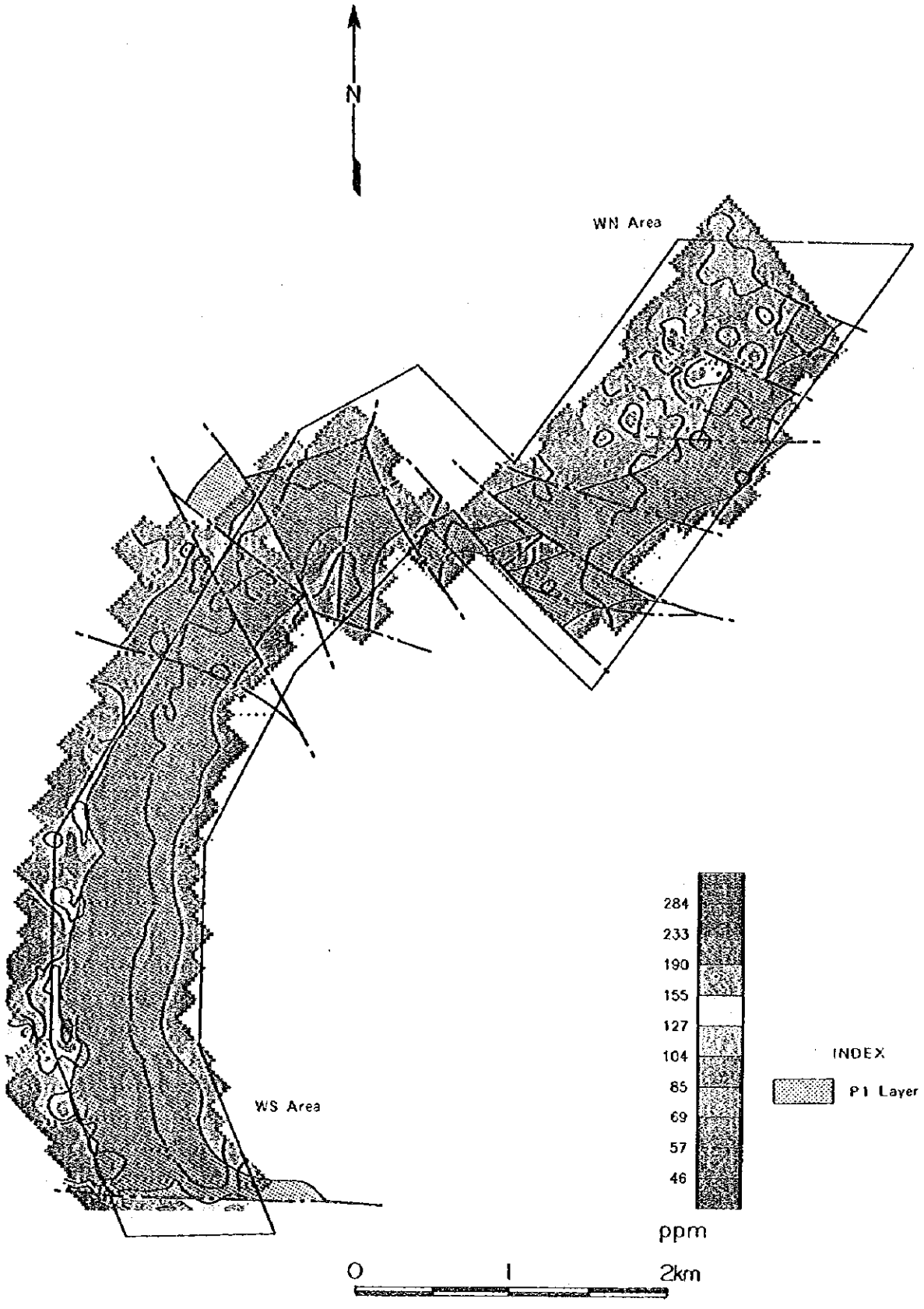

Fig.II-2-10-4 Distribution of Co content (WN, WS area)

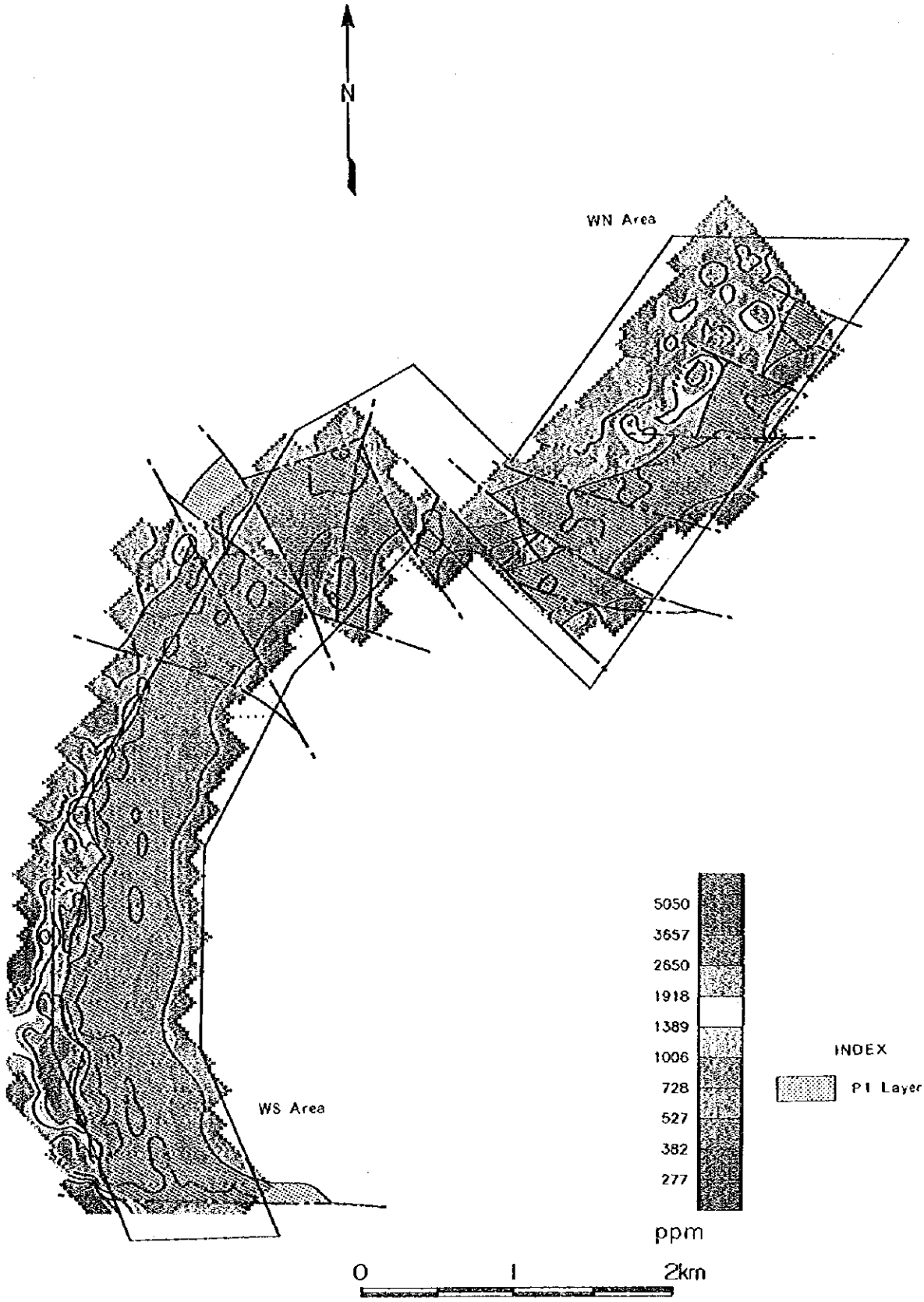

Fig.II-2-10-5 Distribution of Ni content (WN, WS area)

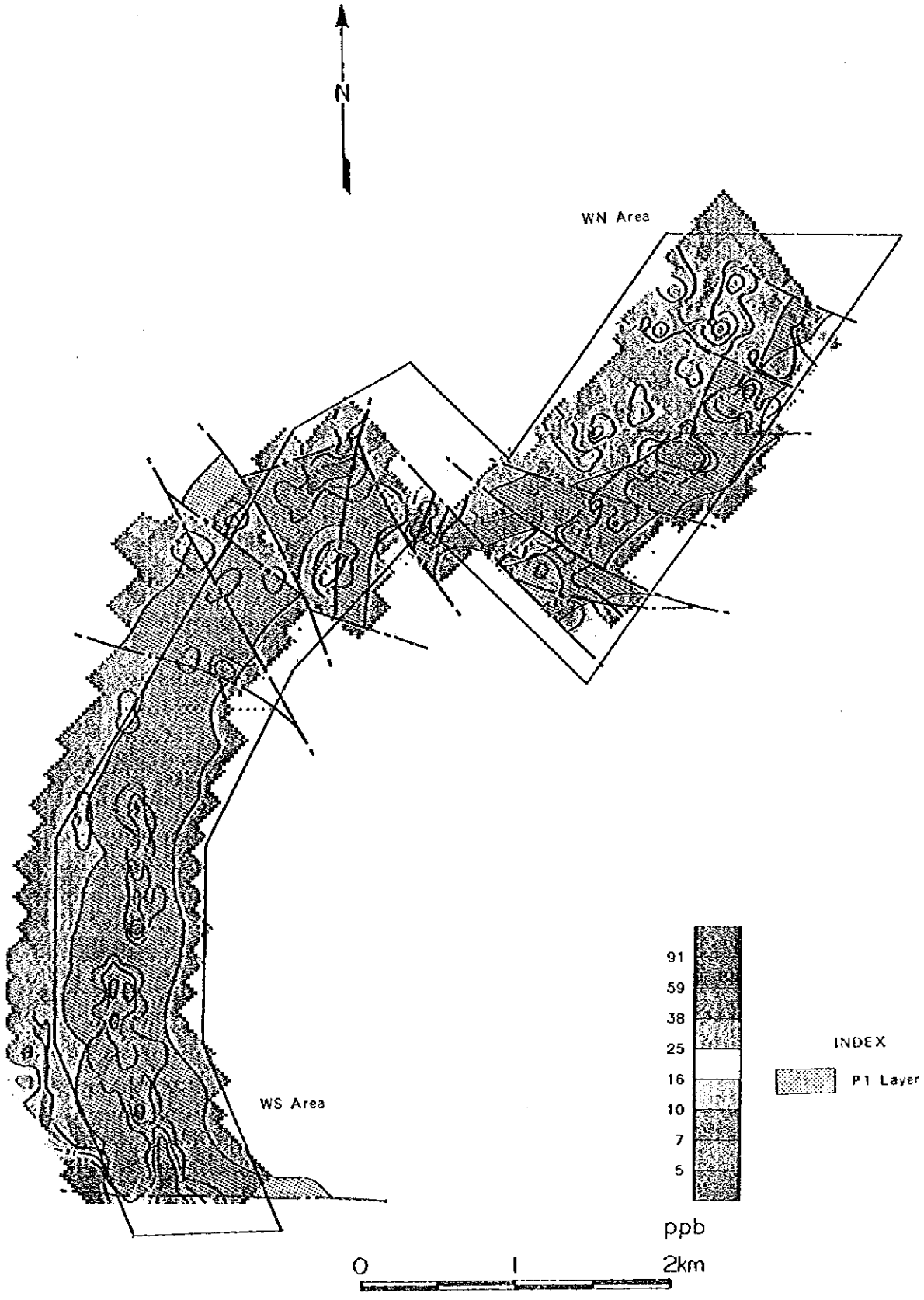

Fig.II-2-10-6 Distribution of Pt content (WN, WS area)

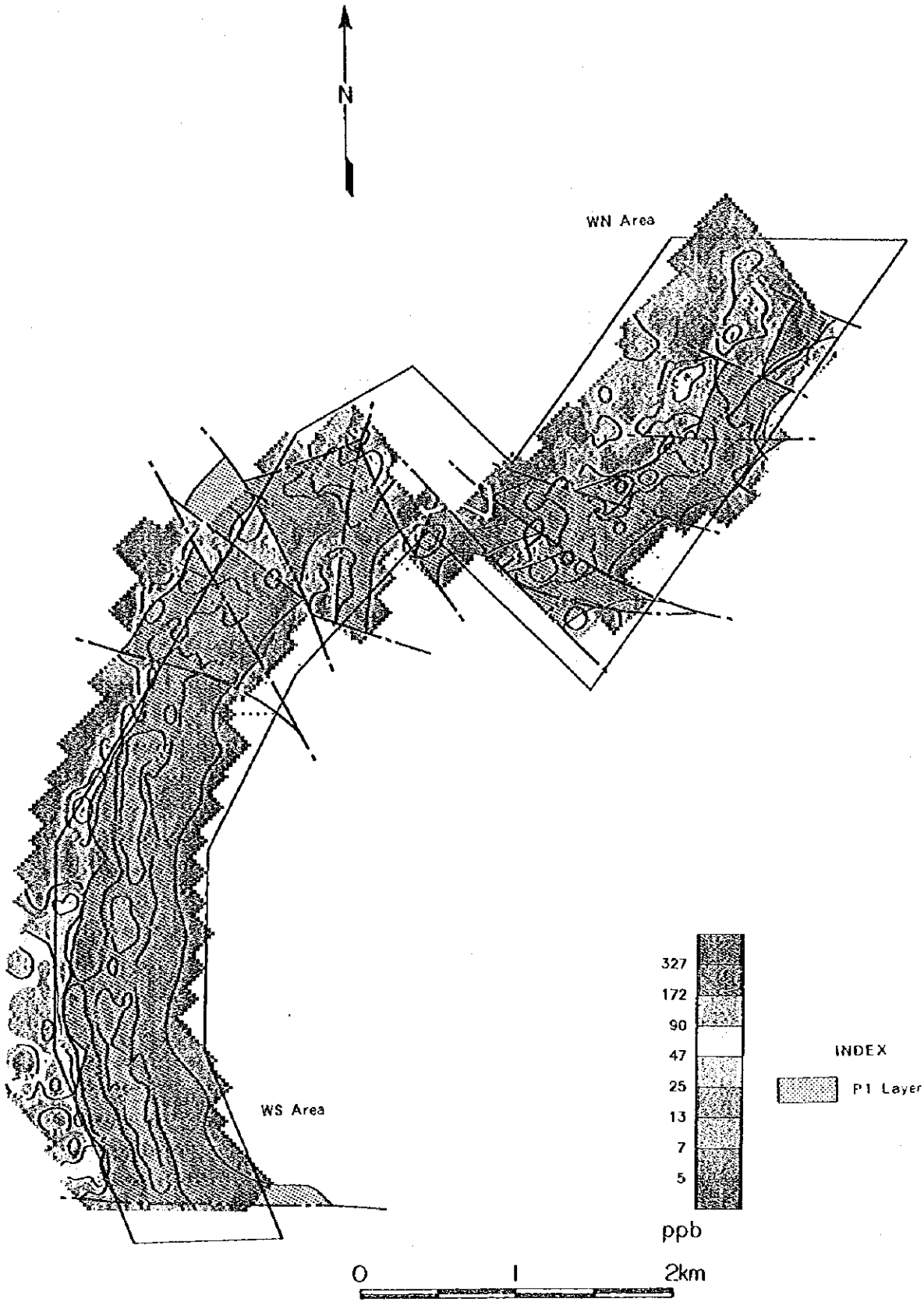

Fig.II-2-10-7 Distribution of Pd content (WN, WS area)

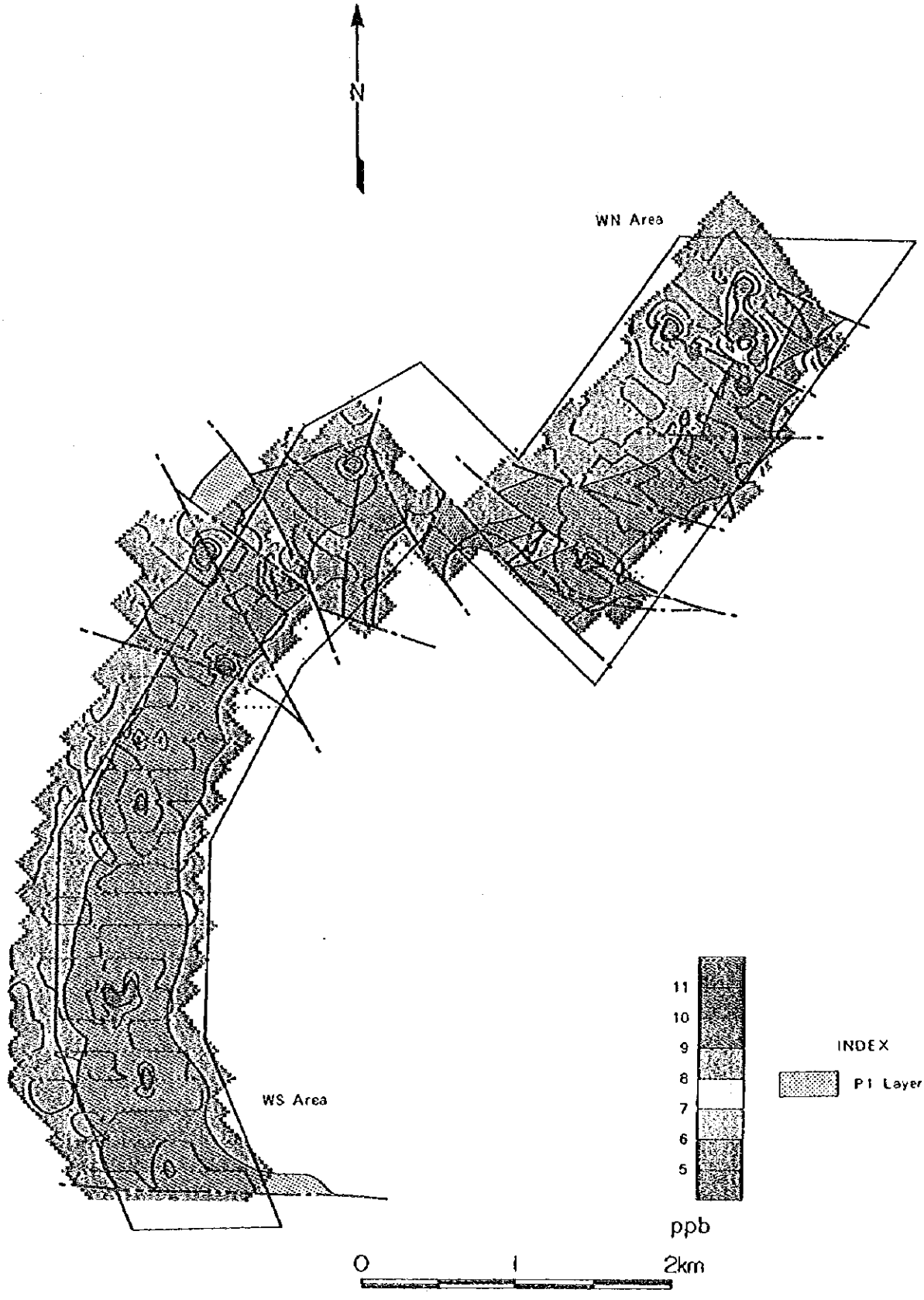

Fig.II-2-10-8 Distribution of Rh content (WN, WS area)

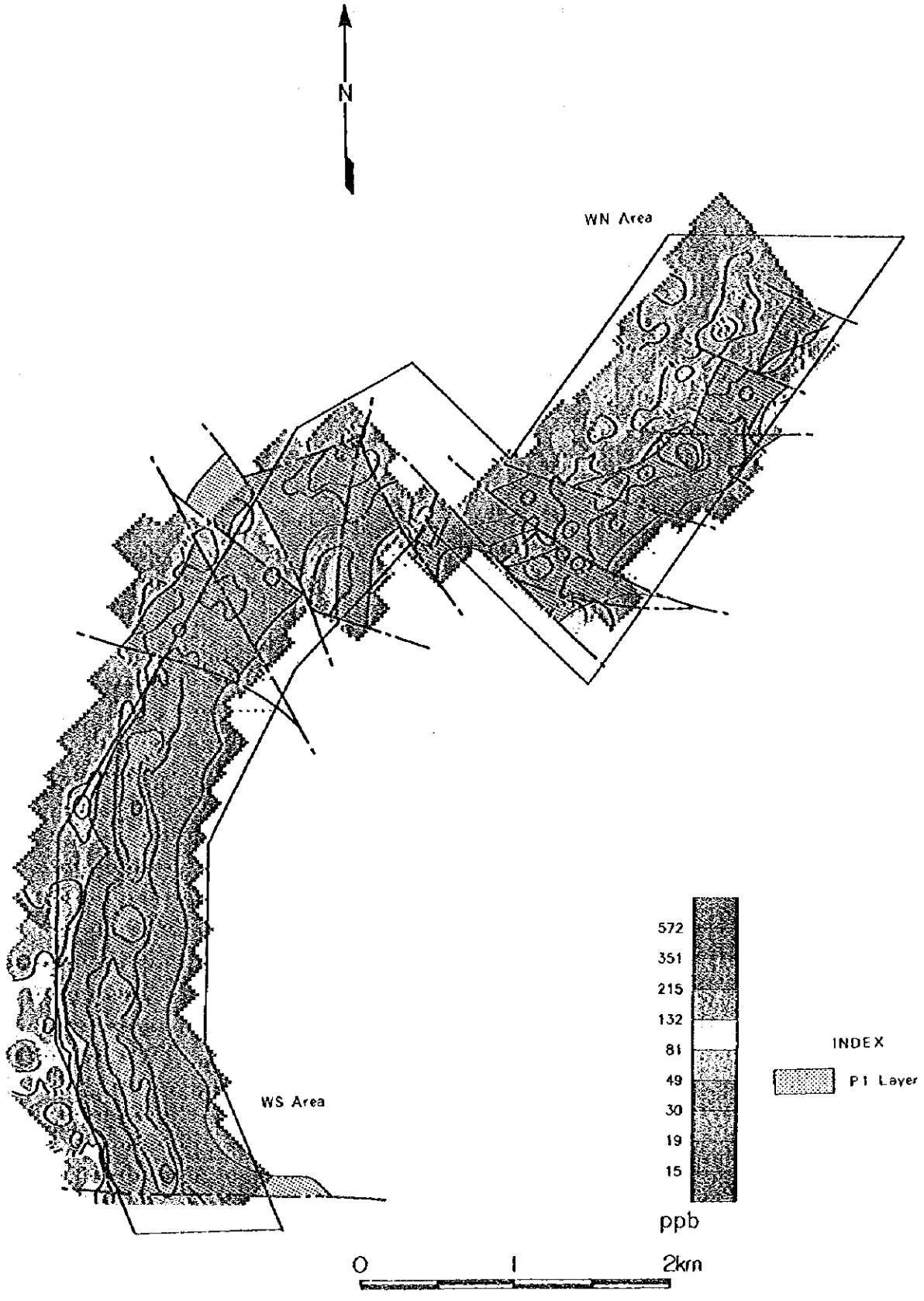

Fig.II-2-10-9 Distribution of PGM content (WN, WS area)

( )

( )

( )

PGM: Comparatively high concentration is continuously recognized between WN01～WN13 and WS01 ～WS17ines, the high cocentration zone above the 1 σ ～2 σ is accompanied,correspond to middle potion of the P1 layer. High concentration is also recognized between WN014～WN23 but the zone is not continuous cutting by fault. the high cocentration zone partly occur in the lower serpentinite.

4. Summary

(1) Metal concentration and geological position

Gold, platinum, and palladium show a narrow continuous distribution, confined to the middle portion of the P1 layer.

Silver and rhodium show low grade and wide a distribution, not corresponding to geology. Silver has no correlation with other elements, suggesting that it has a different condition of concentration compared to these elements. Distribution of the population of Rhodium is difficult because samples shown above the detectable limit are very few.

Copper is devided into 2 clear defferent populations, continuously concentrated in upper portion of P1 layer. Sulphide dissemination which correspond to high copper concentrated zone is recognized in the field, therefore, copper cocentrated zone suggest to existance of mineralization.

Cobalt and nickel show a clear and continuous zone high concentration in the lower portion of P1 layer and lower serpentinite layer. The distribution of cobalt and nickel seem to reflect the geology.

(2) Geological position of metal concentrations.

Geological position of metal concentrations are summarized to Fig.II-2-11.

(3) Comparison of each geochemical survey area

As regard gold and PGM elements, the area expected to high concentration of metals is the WS area, followed by the northeastern portion of the WN area and northern portion of CB area. though the southwestern portion of the WN area is divided into small area by faulting, local metal concentration are recognized. Southern portion of the CB area shows weak metal concentrations, distribution of concentrationsw become patchy. EN and ES areas show no concentration.

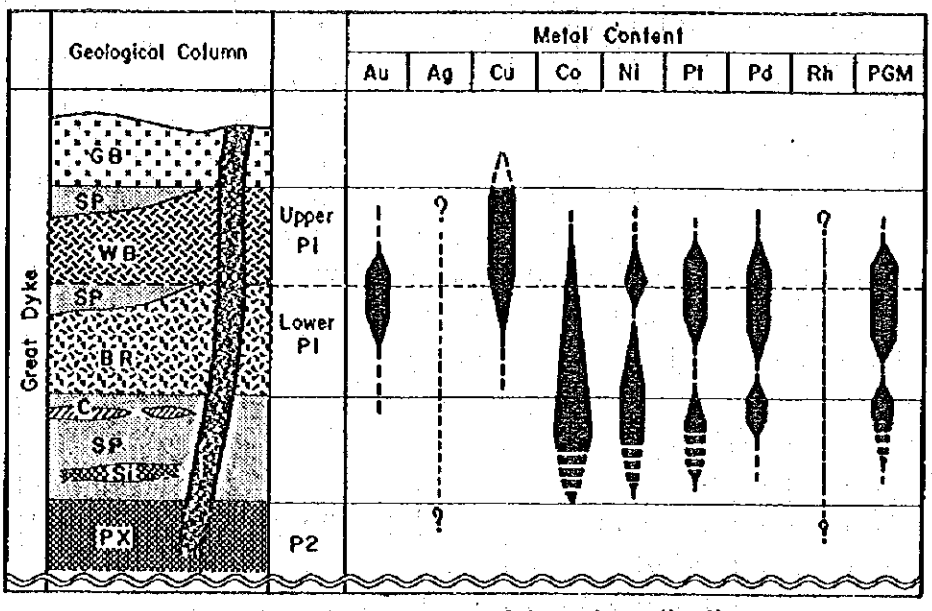

Fig.II-2-11 Summary of the mineralization

Chapter 3 Geophysical survey

3-1 Selection of the Area for Geophysical Survey

The geophysical survey area was determined to the WS area where the distribution of the P1 layer and sulphide mineralization was confirmed by the analysis of the existing data and the field geological survey.

The Location of geophysical survey area is shown in Fig II-3-1, and coordinates of each corner of the area are as follows.

①	S16° 29.29'	E30° 53.41'	②	S16° 29.30'	E30° 54.85'
③	S16° 31.63'	E30° 54.80'	④	S16° 31.60'	E30° 53.34'

3-2 Method of the survey

3-2-1 Content of the survey

An electric prospecting had been carried out using IP method on survey lines.

Specification of geophysical survey is shown in Table II-3-1.

Table II-3-1 Specification of the geophysical survey

Method	Induced polarization method (IP method)
Detection method	Time domain method
Electrode arrangement	Dipole-Dipole
Separation of electrode arrangement	a=100m
Coefficient of electrodes separation	n=1~5
Number of survey line	16
Total length of survey line	32.0km
Tests of physical property of rocks and ores (laboratory test)	35 specimens for chargeability and resistivity

3-2-2 Method of the measurement

1. Determination of survey line and survey

Survey lines established crossing the P1 layer in the WS area. Lines were surveyed using the pocket compass, measuring csron tape and GPS. The base point of survey was set up to the C-23(S16°29.96', E30°54.61') where is the cross point of the road and line C.

The location of survey lines are shown in Fig II-3-2.

2. Electric prospecting (IP method)

1) The principle of IP method

When the electric current is send into the earth, various electro-chemical phenomena occur in the medium which composed the ground.

The following two phenomena are measured by IP method.

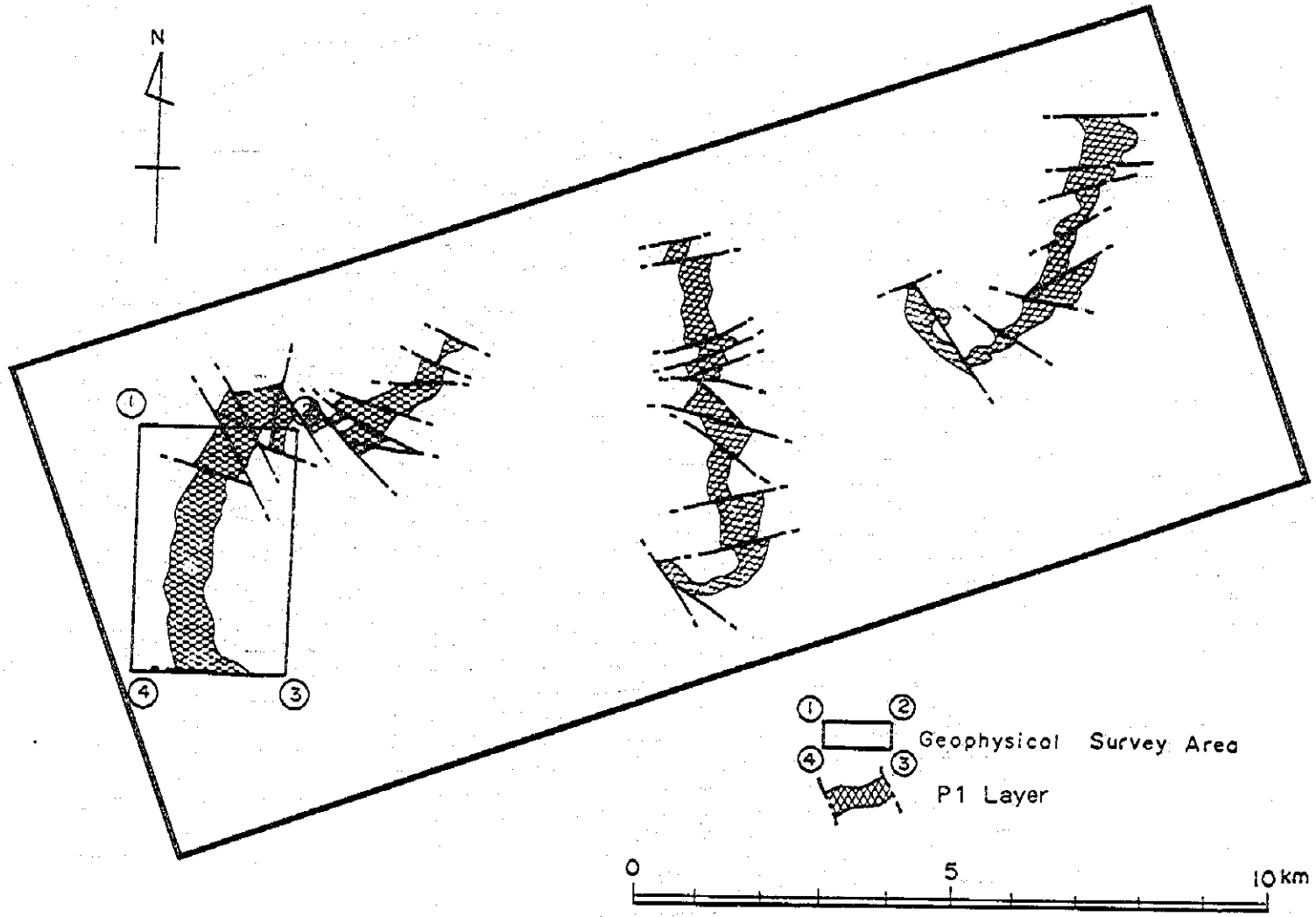

Fig.II-3-1 Locality of the geophysical survey area

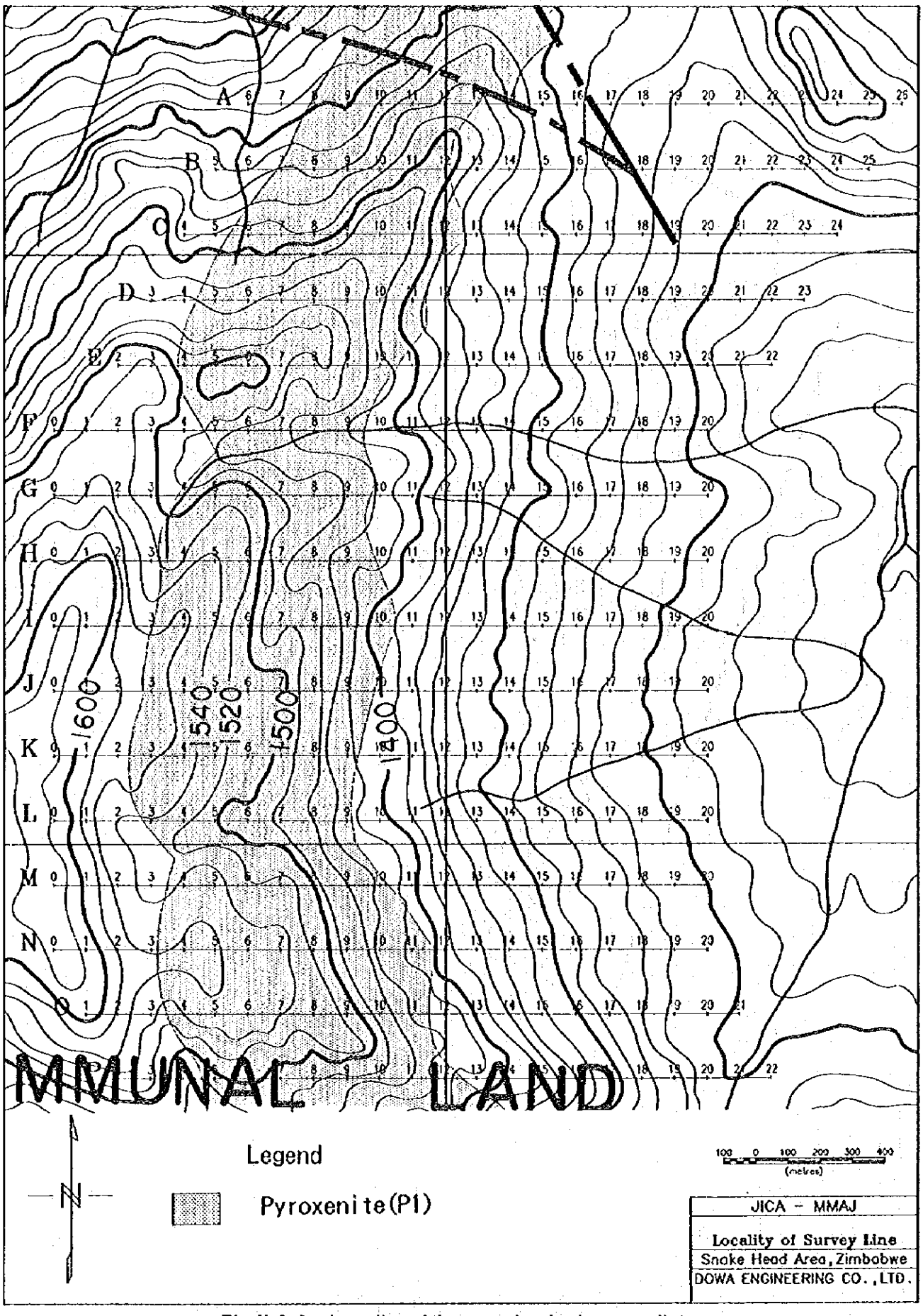

Fig.II-3-2 Locality of the geophysical survey lines

[Over Voltage Effect]

An electric current leads superficially electric double layer on the surface of sulphide and metal conductors. An electric discharge occurs to opposite direction as switching off an electric current. This phenomenon is occurred by the complex effect of ion and electron conduction. This phenomenon results from the mineral with an electron conductivity and is an object of IP survey.

[Normal Effect or Background]

Polarization occurs by sending an electric current in ordinary rocks. This phenomenon results from mainly membrane polarization caused by a small quantity of clay minerals mixed in rocks. The membrane polarization of montmorillonite is the biggest of all of the various clay minerals and that of kaolinite is small. The membrane polarization is maximum when there is 5% clay minerals in volume. However, a membrane polarization decreases when the capacity ratio is larger or smaller than 5%.

The maximum value of membrane polarization is approximately 2% in frequency effect value when there is 5% montmorillonite in volume. This value is extremely small compared with above-mentioned Over Voltage Effect in the sulphide minerals.

2) Measuring method of IP phenomenon

The configuration of measurement is shown in Fig II-3-3.

The measurement had been carried out by the time-domain method. This method (abbreviation symbol T.D. method, transient IP method) sends an intermittent direct current (on/off 2.0sec) into the ground through a couple of current electrode C1,C2. Then two data are measured through the couple of potential electrodes P1,P2. One is the primary voltage(Vp) just before switching off an electric current, the other is the secondary voltage(Vs) during the time(t_4 ~t_{14}) after switching off an electric current.

The concept of the method of measurement is shown in Fig II-3-4 and the list of sampling time is shown Table in II-3-2.

The measurement value of IP effect is generally termed with chargeability, shown as $Vs(t_n)/Vp$[mV/V].

The data of secondary potential difference in this survey has not received an influence of the effect of electromagnetic coupling. At this investigation, we adopted the chargeability in mid-point 935msec data. 1% of chargeability by frequency domain method correspond to 5mV/V of time-domain method respectively.

3. Physical property tests

IP measurement of physical property of 35 specimens that represent rocks and ores in this area has been carried out in order to collect the fundamental data of the electrical characteristics of this area.

These specimens were measured by the time-domain method after cutting them into four faces and soaking in tap water for one day using the same receiver in the field.

4. Measuring equipments and materials

The measuring equipments and materials are shown in Table II-3-3.

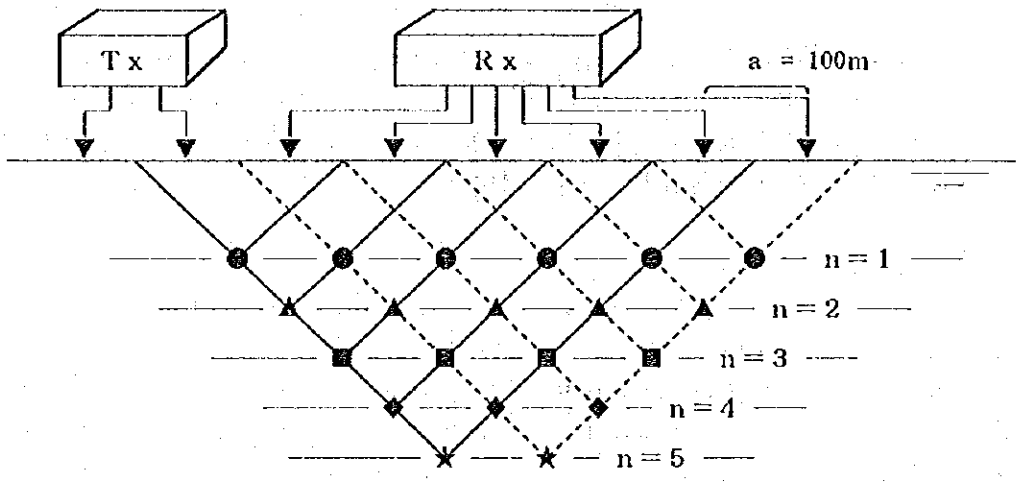

Fig.II-3-3 Configuration of measurement

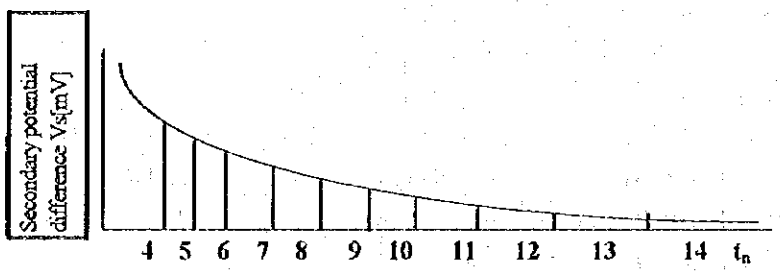

Fig.II-3-4 Concept of the method of measurement

Table II-3-2 List of sampling time

Slice #	4	5	6	7	8	9	10	11	12	13	14
Width (msec)	20	40	40	80	80	140	140	230	230	360	360
Mid-Point (")	60	90	130	190	270	380	520	705	935	1230	1590

Table II-3-3 List of equipments and materials

Field survey

Equipment	Maker	Type	Specification	Amount
Transmitter	IRIS	VIP3000	3000V,5A max. output:3000W Possibility of remote control operation, Standard 220V motor power supply	1
Engine Generator	KUBOTA	AE2200	50Hz 220V 1.9KVA single cylinder 4 cycle	1
Receiver	SCINTREX	IPR-12	8 channel,14 window Input Range:50μV to 14V	1
Electrode		Current electrode Potential electrode	Copper (gauze) $CuSO_4$	1
Cable	Fujikura		VSF1.25mm^{2}cable	1
Survey device	MAGELLAN	NAV5000	Accuracy(positioning:15mRMS(2D mode),speed: +,-0.1knots) Positioning mode: 2D,3D, automatic mode Renewal interval: common 1 sec (2D mode) Speed:0-825knots	1
Measuring compass	Ushikata	Pocket compass	100m Esron tape	4
Communication device	KENWOOD	TH-45G	Output:600mAhW Battery:12V	12

Laboratory test

Transmitter	IRIS	IP-L	Output:1μA ~ 100μA Max. output:10V	1
Receiver	SCINTREX	IPR-12	8channel,14window Input Range:50μV ~ 14V	1
Electrode		Pt		1

3-3 Results of Survey

3-3-1 Section of apparent resistivity and chargeability

Panel diagram of apparent resistivity and chargeability section are shown in Fig II-3-5 to Fig II-3-

6.

A summary of interpretation for distribution of apparent resistivity and chargeability of each section is following.

1. Background value of chargeability was estimated less than 2 mV/V approximately.
2. Chargeability anomaly corresponded to the distribution with Serpentinite is found in the western end of line B~P.
3. Anomalies located in the deep place between stations No.6 to No.10 of E,H,I,J,K,L,M lines suggest the existence of deep anomaly source.
4. Distribution of apparent resistivity shows low resistivity in shallow place and have tendency to increase resistivity in deeper place.
5. The distribution area of Gabbro shows slightly apparent low resistivity. Classification depending on a resistivity between Pyroxenite and Serpentinite is not clear.
6. Chargeability anomaly is not found at the week Sulphide dissemination zone.

Distributions of resistivity and chargeability and relationship in each section were summarized as follows.

Line A

Resistivity shows less than 100 Ω·m in shallow part at the station No.8,15,16,19, and have tendency to shows high resistivity in deep part. It is considered that the low resistivity at the shallow part results from the weathering, argillization, alteration, slightly crack and moisture condition.

Chargeability shows monotonous distribution less than 2.5 mV/V, and remarkable anomaly pattern isn't admitted.

Line B

Resistivity shows less than 100Ω·m in shallow part in the western side of station No.9 and between stations No.17 and No.20, and have tendency to show high resistivity in deep part.

Chargeability shows a weak anomaly with 3.7mV/V in deep part , between stations No8 and No.9. Pyroxenite distributes on the surface of this area, but it is estimated that lower Serpentinite layer may be distributes around the anomaly. The other chargeability anomaly with maximum 3.5mV/V recognized in shallow part between stations No.22 and No.24, but low resistivity anomaly is not recognized at same place. This place corresponds to the Gabbro.

Line C

Resistivity shows less than 100 Ω·m in shallow part at station No.11, between stations No.14 and No.16 and the eastern side from the station No.20.

Chargeability shows anomaly with maximum 4.3mV/V around the western end of the line, between stations No.6 and No.9. This area corresponds to the Serpentinite. Other weak anomaly with 2.6mV/V is recognized in shallow part between stations No.20 and No.23.

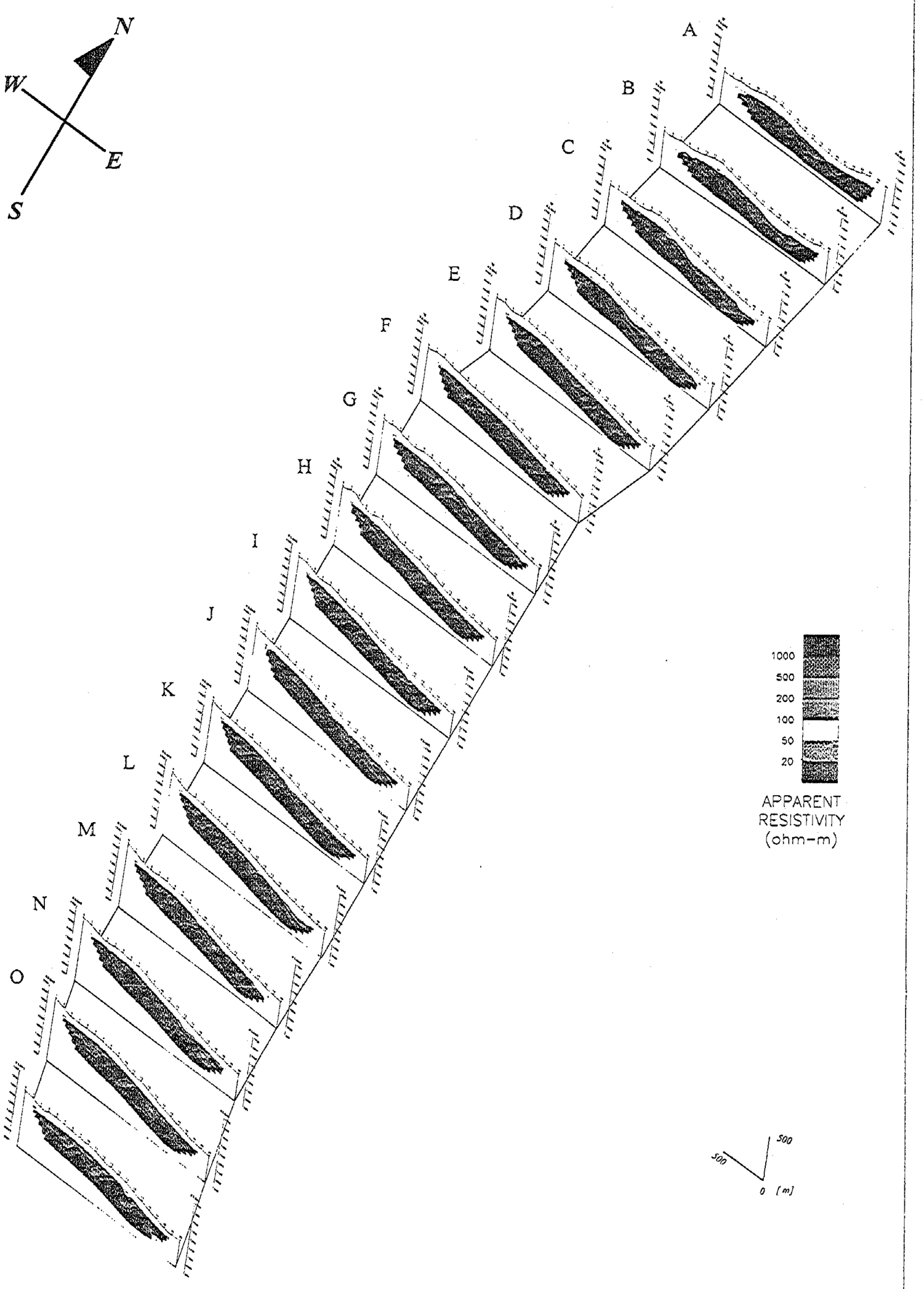

Fig.II-3-5 Panel diagram of apparent resistivity section

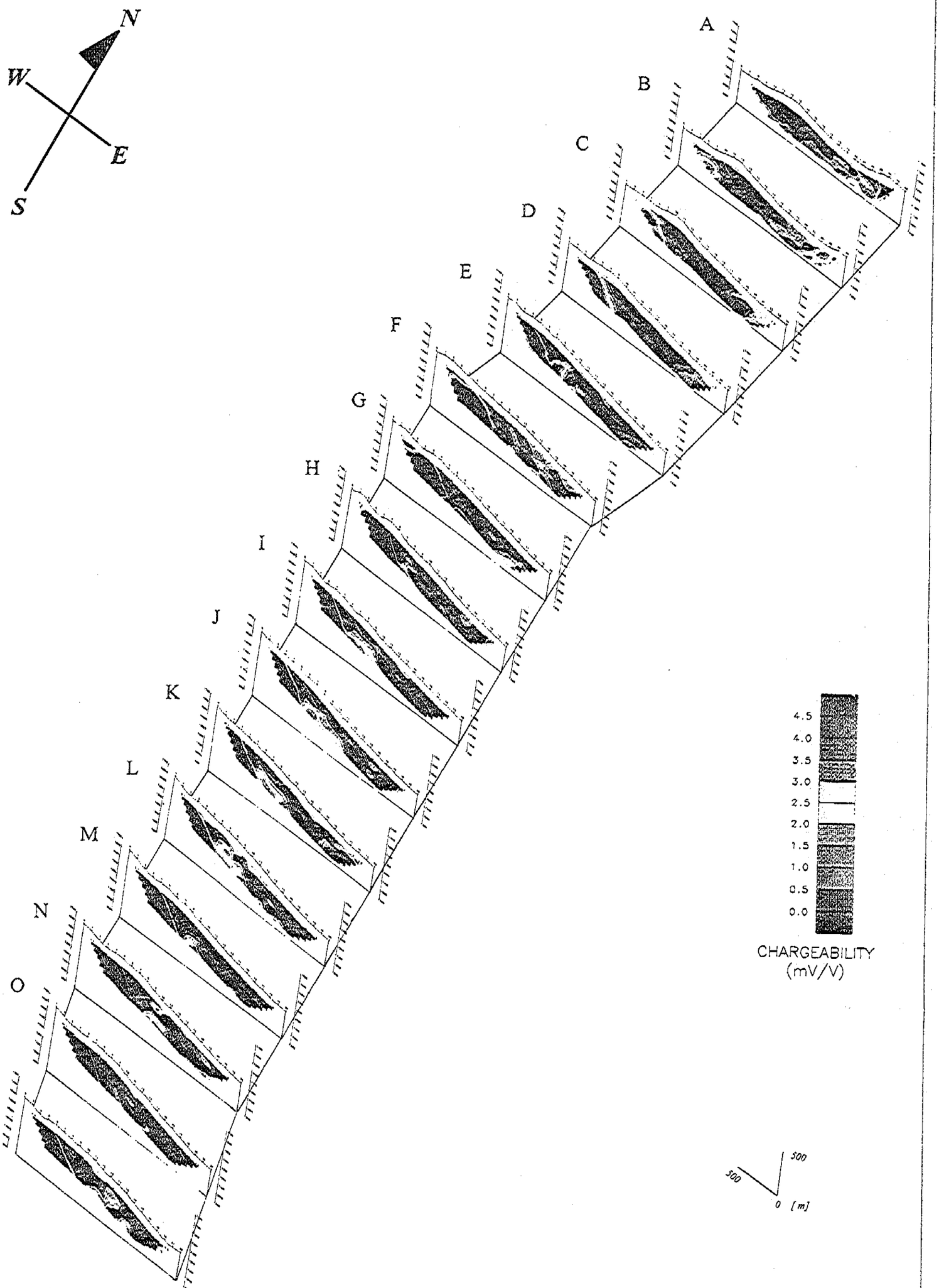

Fig.II-3-6 Panel diagram of chargeability section

Line D

Resistivity shows less than 100 Ω·m in shallow part between stations No.12 and No.14.

Chargeability shows anomaly pattern with maximum 19.5mV/V between stations No.4 and No.8. An anomaly distribution form, suggest to exist an anomaly source in shallow part. This position of anomaly corresponds to Serpentinite.

Line E

Resistivity almost shows 200~1500 Ω·m except for the shallow part between stations No.11 and No.15. General view of the resistivity distribution shows 200~500 Ω·m in the distribution area of Gabbro, and shows 500~1000 Ω·m in the lower Pyroxenite area.

Chargeability shows an apparent anomaly pattern around the station No.3 and No.5. This position corresponds to distribution area of Serpentinite. At east side of this anomaly pattern the other anomaly with the maximum 5.1mV/V is recognized in the deep part at the satiation No.9.

Line F

Resistivity generally shows 200~2000 Ω·m. High resistivity can be found in the deep part.

Chargeability shows an apparent pants leg pattern with maximum 9.3mV/V in the deep part between stations No.2 and No.7. An anomaly distribution form suggest to exist an anomaly source in deep depth. The position of an anomaly source corresponds to the extension of Serpentinite.

Line G

Resistivity generally shows 200~1300. Ω·m. This line has a tendency to be higher resistivity in the deep part.

Chargeability shows an apparent pants leg pattern around the station No.4,5. An anomaly distribution form suggest to exist an anomaly source in subsurface. A minus chargeability below the stations No.6~9 consider to be a result depending on IP anomaly influence of above-mentioned No.4,5. Chargeability shows a background value less than 2mV/V in the eastern side from station No.11.

Line H

Resistivity distribution almost similar to the line H.

Chargeability shows an apparent pants leg pattern around the station No.3~4. An anomaly distribution form suggest to exist an anomaly source in subsurface. This anomaly source corresponds to the distribution area of Serpentinite. The other weak anomaly with 3mV/V is recognized in deep part below the stations No.7 and No.8. But accompanied with low resistivity anomaly.

Line I

Resistivity generally shows 200~1500 Ω·m.

Chargeability shows an apparent pants leg pattern around the station No.2,3. An anomaly distribution form suggest to exist an anomaly source in comparatively deep place. In the east side of this

anomaly pattern, an weak anomaly with maximum 3.6mV/V is recognized in the deep part . Chargeability shows a background value less than 2mV/V in the eastern side from the station No.10.

Line J

Resistivity distribution almost similar to the line I.

Chargeability shows an apparent pants leg pattern around the station No.1,2. An anomaly distribution form suggest to exist an anomaly source in subsurface. Other weak anomaly with maximum 3.9mV/V is recognized in deep part between stations No.6 and No.11. This anomaly suggests a deep anomaly source continued from the line I.

Line K

Resistivity distribution almost similar to the line J.

Chargeability shows an apparent half of pants leg pattern around the station No.1~3. An anomaly distribution form suggest to exist an anomaly source in subsurface. Other weak but an apparent anomaly with maximum 3.7mV/V is recognized in deep part between stations No.6 and No.11. This anomaly shows similar form to the line I,J and may be caused by same continuous anomaly source.

Line L

Resistivity distribution almost similar to that of the line K. Remarkable anomaly is not recognized.

Chargeability shows an apparent half of pants leg pattern around the station No.1,2. This position of anomaly corresponds to the distribution area of Serpentinite. Other weak anomaly similar to the line I,J,K is recognized in deep part between stations No.6 and No.9. Chargeability in eastern side from the station No.9 shows a background value with 2mV/V.

Line M

Resistivity distribution almost similar to the line L. Remarkable anomaly is recognized.

Chargeability shows an apparent half of pants leg pattern around the station No.2,3. An anomaly distribution form suggest to exist an anomaly source in subsurface. This position of anomaly corresponds to the distribution area of Serpentinite. Other weak anomaly with maximum 2.3mV/V is recognized in deep part between stations No.8 and No.10.

Line N

Resistivity generally shows 200~3000 Ω·m except for the distribution area of Gabbro.

Chargeability shows an apparent half of pants leg pattern around the station No.2~3. An anomaly distribution form suggest to exist an anomaly source in subsurface. This position of anomaly corresponds to the distribution area of Serpentinite. An independent weak anomaly in shallow to deep part between stations No9 and No.10. may be reflected very sectional anomaly source located in subsurface.

Line O

Resistivity generally shows 200~2000 Ω·m. High resistivity excels in deep part.

Chargeability shows an apparent half of pants leg pattern around the station No.3,4. An anomaly distribution form suggest to exist an anomaly source in subsurface. This position of anomaly corresponds to the distribution area of Serpentinite.

Line P

Resistivity generally shows 200~2000 Ω·m. High resistivity excels in deep part.

Chargeability shows an apparent half of pants leg pattern around the station No.5,6. An anomaly distribution form suggest to exist an anomaly source in subsurface.

3-3-2 Plan of apparent resistivity and chargeability

The plan of apparent resistivity and chargeability for this survey are shown in Fig II-3-7 and Fig II-3-8. In the section, Chargeability anomaly pattern by dipole-dipole electrode arrangement can be displayed the pants leg pattern. This pattern cutting "n" level of the coefficient of electrodes separation, appear both side of expected anomaly source on the plan. An anomaly pattern changes it's distribution increasing "n" level and not become correspond to anomaly source. Therefore, the relationship between geophysical anomalies, expected anomaly source and geological situation were discussed using plan of n=1 level in the case of shallow place, and n=4,5 level in the case of deeper place.

The distribution of apparent resistivity

n=1

Plan of n=1 level shows resistivity situation in subsurface. This figure shows low resistivity zone less than 100 Ω·m in the north and east area. The area where generally shows less than 200 Ω·m corresponds to the distribution area of Gabbro.

n=2,3,4,5

The distribution of apparent resistivity deeper than n=2 level shows more than 200 Ω·m and high resistivity predominate in the deep part. Remarkable low resistivity anomaly can not be recognized.

The distribution of chargeability

n=1

At the west side of survey area, a chargeability anomaly is continuously admitted from the line C to the line P. This anomaly shows chargeability with maximum 26.5mV/V, that position corresponds to the distribution area of Serpentinite with chromite. We are thought that chargeability anomaly of n=1 level may be reflected by anomaly source near the subsurface. This anomaly source is consider to have high resistivity and high chargeability, because of low resistivity anomaly isn't admitted with same position.

n=4,5

Weak chargeability anomaly (2~5mV/V) is continuously recognized between stations No.6 and No.10 on the line E, and from line H to N.

( )

( )

( )

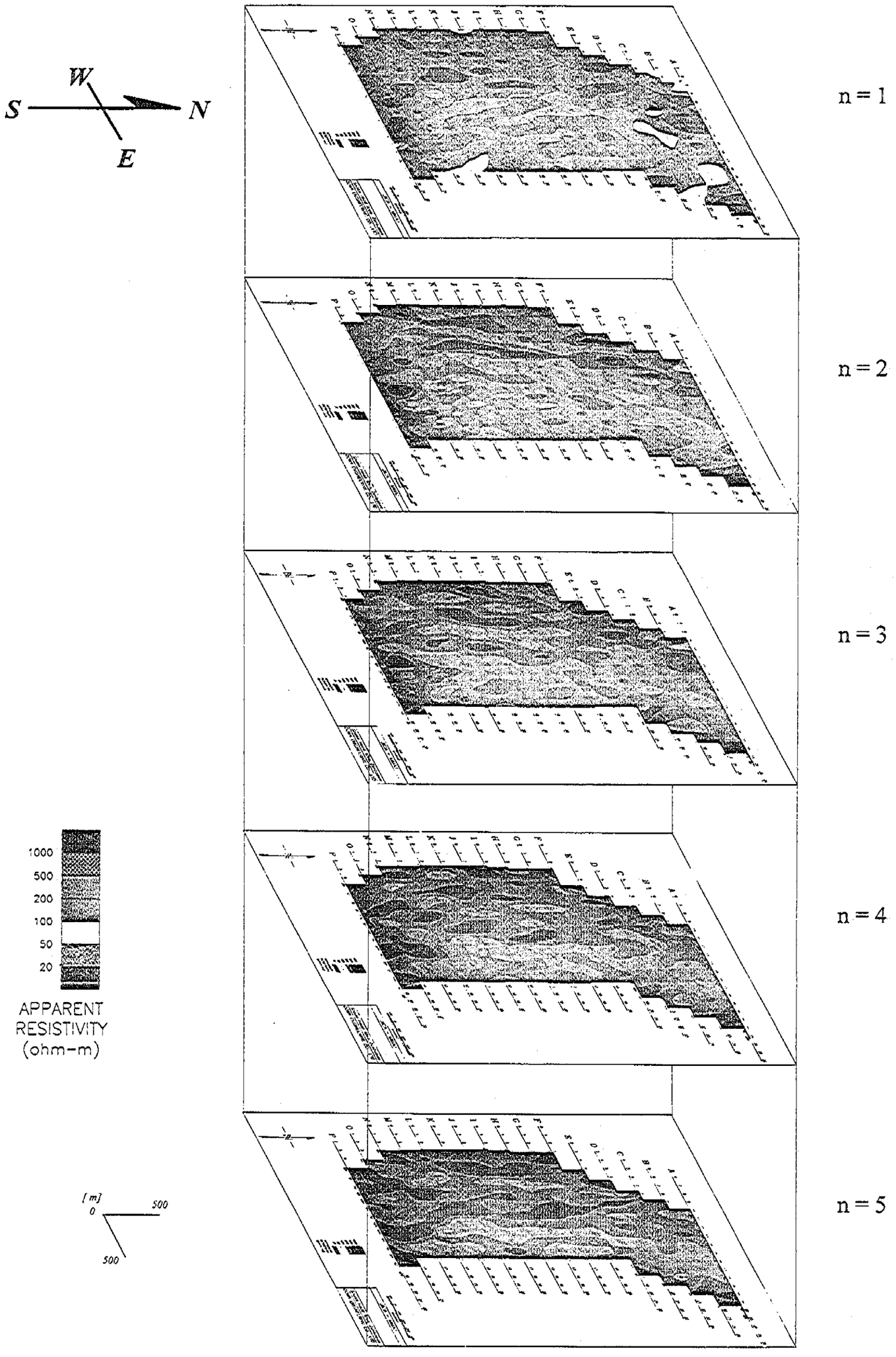

Fig.II-3-7 Panel diagram of apparent resistivity plan

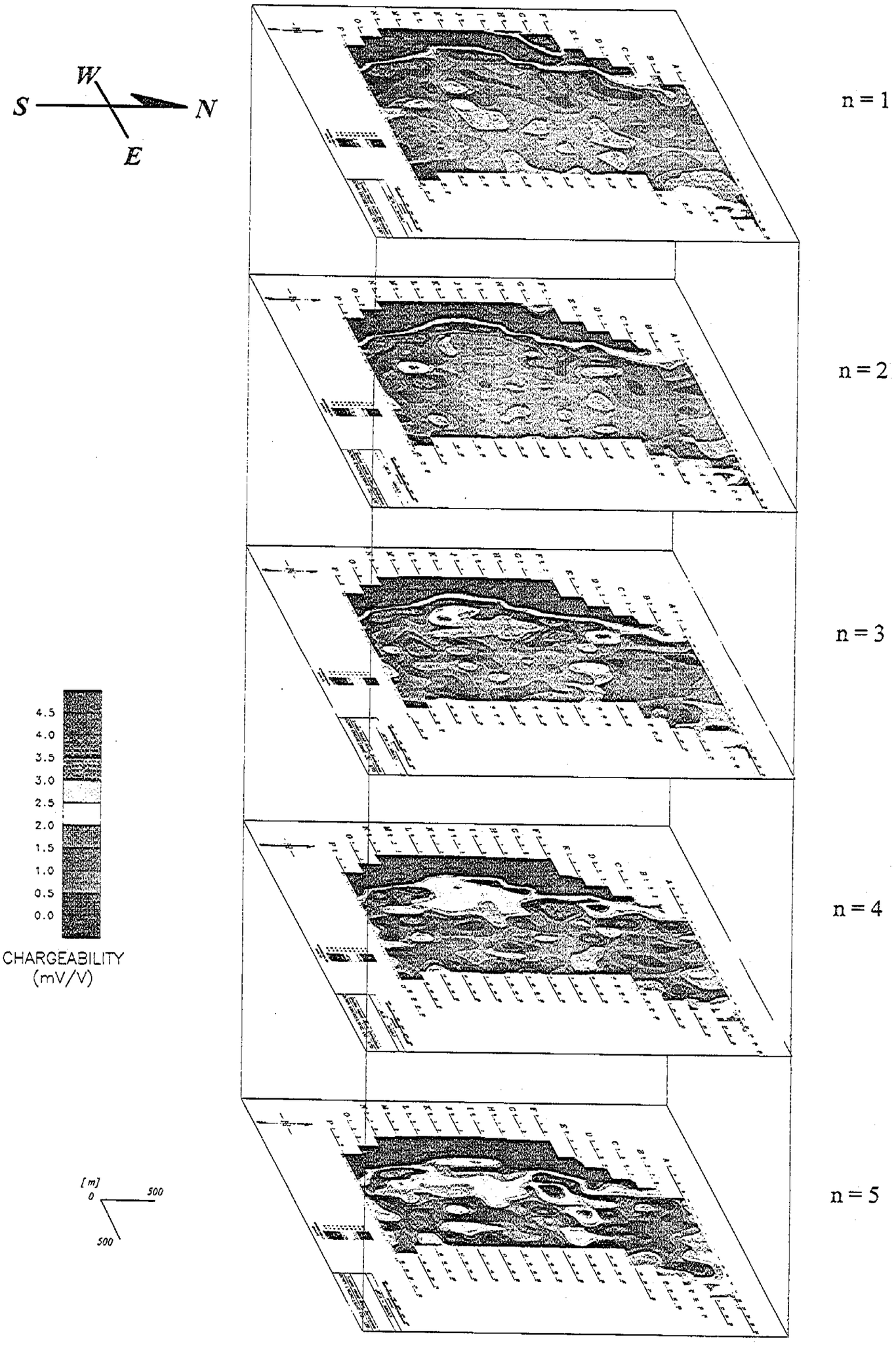

Fig.II-3-8 Panel diagram of chargeabiliry plan

3-3-3 Summary

Characteristics of chargeability distribution are summarized in Table II-3-4.

Table II-3-4 Summary of geophysical survey

Line	Resistivity[Ω·m]	Chargeability[mV/V]	Characteristic of distribution
A	67~1,277	0.1~2.4	Monotonous distribution less than 2.4mV/V.
B	52~1,196	0.1~3.7	Deep and weak anomaly 3.7mV/V between stations No.8 and No.9.
C	63~1,533	0.3~4.3	Maximum 4.3mV/V between stations No.6 and No.9.
D	86~1,704	-0.9~11.2	Anomaly between stations No.4 and No.8.
E	150~1,284	-0.1~16.4	Anomaly between stations No.3 and No.5. Deep and weak anomaly between stations No8 and No.10.
F	127~1,955	-0.7~9.3	Anomaly between stations No.2 and No.7.
G	110~1,264	-1.8~11.2	Anomaly in the station No.4,5.
H	134~1,462	-0.5~12.4	Anomaly between stations No.3 and No.4. Deep and week anomaly in the station No.7,8.
I	110~1,934	-0.4~11.5	Anomaly in the station No.2,3. Deep and week anomaly between stations No.6 and No.10.
J	19~1,815	-0.6~12.0	Anomaly in the station No.1,2. Deep and week anomaly between stations No.6 and No.11.
K	113~2,167	0.0~16.6	IP anomaly with half of pants leg pattern between stations No.1~3. deep and week anomaly between stations No.6~9.
L	98~2,448	-0.1~13.1	IP anomaly with half of pants leg pattern in the station No.1,2. deep and week anomaly between stations No.6~9.
M	75~1,594	-0.8~14.1	IP anomaly with half of pants leg pattern in the station No.2,3. deep and week anomaly between stations No.8 and No.10.
N	80~3,447	-1.4~26.5	IP anomaly half of pants leg pattern between stations No.2~3. deep and week anomaly in the station No.9,10.
O	154~2,102	-1.2~16.0	IP anomaly half of pants leg pattern in the station No.3,4.
P	60~3,709	-1.9~9.8	IP anomaly half of pants leg pattern in the station No.5,6.

3-4 Physical Properties of Rocks and Ore Samples

Results of physical property tests are presented in Table II-3-5. Statistics of physical properties are presented in Table II-3-6. Relationship between chargeability and resistivity of the rock and ore samples are shown in Fig II-3-9.

These samples range in resistivity from 657 (Serpentinite) to 48,974 Ω·m (dolerite) and range in chargeability from maximum 49.5mV/V(Serpentinite) to 0.6mV/V(Dolerite).

Anisotropy of physical property in rocks was not recognized both in resistivity and in

Table II-3-5 Results of physical property tests (1)

No.	Sample No.	Rock Type	Rem.		Resistivity (ohm-m)	Chargeability (mV/V)										
						M4	M5	M6	M7	M8	M9	M10	M11	M12	M13	M14
1	E17	Dolerite		X	43,974	7.0	5.1	3.9	2.9	2.1	1.5	1.1	0.8	0.6	0.4	0.3
				Y	44,287	9.0	6.7	5.1	3.9	2.9	2.1	1.6	1.2	0.8	0.6	0.4
				Z	41,795	7.7	5.6	4.2	3.1	2.3	1.7	1.2	0.9	0.6	0.4	0.3
2	E11	Gabbro		X	8,888	239	210	185	160	136	115	97	80	66	53	43
				Y	5,678	236	207	183	158	135	114	96	80	66	54	43
				Z	7,739	257	226	200	173	148	126	106	88	73	59	48
3	E12	Gabbro		X	7,475	159	139	122	105	90	76	64	53	44	36	29
				Y	7,167	159	139	122	106	90	77	65	54	45	37	30
				Z	8,262	162	142	125	108	93	78	66	55	45	37	30
4	I11	Gabbro		X	7,867	236	208	183	158	136	115	97	80	66	54	44
				Y	6,788	188	163	143	124	106	90	75	62	51	42	34
				Z	10,941	215	188	165	143	122	103	87	72	59	49	39
5	I20	Gabbro		X	7,734	145	127	111	96	82	70	59	49	40	33	27
				Y	5,075	126	109	95	82	70	59	49	41	34	27	23
				Z	4,885	126	109	96	83	70	59	50	41	34	28	23
6	M11	Gabbro		X	6,538	152	133	117	102	88	75	63	53	44	36	30
				Y	7,822	132	115	101	87	75	63	53	44	36	30	24
				Z	6,970	150	131	114	98	84	71	59	49	40	33	26
7	E5	Pyroxenite	Sulphide	X	15,887	8.1	6.9	5.9	5.0	4.2	3.4	2.8	2.3	1.9	1.5	1.2
				Y	16,444	8.7	7.4	6.4	5.4	4.5	3.7	3.1	2.5	2.0	1.6	1.3
				Z	13,973	7.2	6.1	5.2	4.4	3.7	3.1	2.5	2.0	1.6	1.3	1.0
8	E6	Pyroxenite	Sulphide	X	16,511	7.8	6.6	5.7	4.8	4.0	3.3	2.7	2.2	1.7	1.4	1.1
				Y	18,462	6.9	5.8	4.9	4.1	3.4	2.8	2.3	1.8	1.5	1.1	0.9
				Z	15,581	8.2	6.9	6.0	5.0	4.2	3.5	2.8	2.3	1.9	1.5	1.2
9	E9	Pyroxenite	Sulphide	X	13,034	7.6	6.5	5.5	4.7	3.9	3.3	2.7	2.2	1.8	1.4	1.1
				Y	16,430	9.4	8.0	6.9	5.8	4.9	4.0	3.3	2.7	2.2	1.8	1.4
				Z	14,415	9.3	7.9	6.8	5.7	4.8	4.0	3.3	2.7	2.2	1.7	1.4
10	E10.5	Pyroxenite	Sulphide	X	3,462	8.2	6.6	5.4	4.4	3.5	2.8	2.3	1.8	1.4	1.1	0.8
				Y	6,139	10.5	8.8	7.5	6.2	5.1	4.2	3.4	2.8	2.2	1.8	1.4
				Z	4,898	9.5	7.9	6.6	5.5	4.5	3.7	3.0	2.4	1.9	1.6	1.2
11	E10	Pyroxenite	Sulphide	X	27,167	7.3	6.0	5.0	4.2	3.4	2.8	2.2	1.8	1.4	1.1	0.8
				Y	21,551	6.3	5.2	4.4	3.6	2.9	2.4	1.9	1.5	1.2	0.9	0.7
				Z	27,634	5.7	4.7	3.9	3.2	2.5	2.0	1.6	1.3	1.0	0.7	0.6
12	I9	Pyroxenite	Sulphide	X	15,915	10.0	8.8	7.4	6.3	5.3	4.5	3.7	3.0	2.5	2.0	1.6
				Y	15,156	9.7	8.3	7.2	6.2	5.2	4.4	3.6	3.0	2.4	2.0	1.6
				Z	14,504	9.5	8.1	6.9	5.9	4.9	4.1	3.4	2.7	2.2	1.8	1.4
13	E2	Pyroxenite		X	4,570	17.0	14.6	12.5	10.6	8.9	7.4	6.1	5.0	4.1	3.3	2.6
				Y	4,840	17.2	14.7	12.7	10.8	9.1	7.5	6.2	5.1	4.1	3.3	2.7
				Z	11,018	17.6	15.1	13.0	11.0	9.3	7.7	6.4	5.2	4.2	3.4	2.7
14	E7	Pyroxenite		X	15,151	7.8	6.6	5.7	4.9	4.1	3.4	2.9	2.3	1.9	1.5	1.2
				Y	12,485	9.1	7.8	6.8	5.9	5.0	4.2	3.5	2.9	2.4	1.9	1.6
				Z	18,521	10.4	8.9	7.6	6.7	5.7	4.8	4.0	3.3	2.7	2.2	1.8
15	E8	Pyroxenite		X	9,512	12.3	10.6	9.2	7.8	6.6	5.5	4.6	3.8	3.1	2.5	2.0
				Y	10,586	10.5	9.0	7.8	6.7	5.7	4.7	3.9	3.2	2.6	2.1	1.7
				Z	11,024	11.6	10.0	8.7	7.5	6.3	5.3	4.4	3.7	3.0	2.4	2.0
16	M4	Pyroxenite		X	18,504	9.4	8.0	6.9	5.9	4.9	4.1	3.4	2.8	2.3	1.8	1.5
				Y	15,401	10.4	8.8	7.6	6.5	5.5	4.6	3.8	3.1	2.6	2.1	1.7
				Z	24,516	8.2	6.9	5.9	5.0	4.2	3.5	2.9	2.4	2.0	1.6	1.3
17	M5	Pyroxenite		X	22,091	8.9	7.5	6.4	5.4	4.5	3.7	3.0	2.5	2.0	1.6	1.2
				Y	20,063	10.3	8.7	7.5	6.3	5.3	4.4	3.6	2.9	2.4	1.9	1.5
				Z	19,060	8.8	7.4	6.3	5.3	4.4	3.7	3.0	2.4	2.0	1.6	1.2
18	M6	Pyroxenite		X	39,328	6.0	4.9	4.2	3.5	2.9	2.4	1.9	1.6	1.3	1.0	0.8
				Y	31,273	5.5	4.5	3.8	3.2	2.6	2.1	1.7	1.4	1.1	0.9	0.7
				Z	27,203	5.7	4.7	3.9	3.3	2.7	2.2	1.8	1.5	1.2	0.9	0.7

Table II-3-5 Results of physical property tests (2)

No.	Sample No.	Rock Type	Rem.		Resistivity (ohm-m)	Chargeability (mV/V)										
						M4	M5	M6	M7	M8	M9	M10	M11	M12	M13	M14
19	M7	Pyroxenite		X	20,474	11.3	9.6	8.3	7.1	6.0	5.0	4.2	3.5	2.8	2.3	1.9
				Y	23,636	11.6	9.4	8.2	7.0	5.9	5.0	4.1	3.4	2.8	2.3	1.8
				Z	18,164	9.5	8.4	7.3	6.2	5.2	4.4	3.7	3.0	2.4	2.0	1.6
20	M8	Pyroxenite		X	8,313	12.7	11.0	9.6	8.3	7.2	6.1	5.2	4.3	3.6	3.0	2.5
				Y	10,425	14.0	12.2	10.8	9.2	7.8	6.6	5.6	4.6	3.8	3.2	2.5
				Z	7,742	12.2	10.6	9.2	8.0	6.9	5.8	4.9	4.1	3.4	2.8	2.3
21	M9	Pyroxenite		X	16,950	20.9	18.3	16.1	13.9	11.9	10.1	8.5	7.1	5.9	4.8	4.0
				Y	15,116	21.1	18.5	16.3	14.1	12.1	10.2	8.6	7.2	5.9	4.8	4.0
				Z	15,921	19.1	16.7	14.7	12.6	10.8	9.2	7.7	6.4	5.3	4.3	3.5
22	I10	Pyroxenite		X	7,841	13.6	11.9	10.4	9.0	7.7	6.5	5.4	4.5	3.7	3.0	2.5
				Y	7,267	12.7	11.1	9.7	8.3	7.1	6.0	5.0	4.2	3.4	2.8	2.3
				Z	8,109	12.4	10.7	9.4	8.0	6.8	5.8	4.8	4.0	3.3	2.7	2.2
23	I4	Pyroxenite		X	19,435	4.7	3.8	3.2	2.6	2.1	1.7	1.4	1.1	0.8	0.6	0.5
				Y	17,359	4.5	3.6	3.0	2.5	2.0	1.6	1.3	1.0	0.8	0.6	0.4
				Z	16,337	4.1	3.3	2.7	2.3	1.8	1.5	1.2	0.9	0.7	0.5	0.4
24	I5	Pyroxenite		X	24,326	5.6	4.6	3.9	3.3	2.7	2.2	1.8	1.4	1.2	0.9	0.7
				Y	18,963	5.8	4.8	4.1	3.4	2.8	2.3	1.9	1.5	1.2	1.0	0.8
				Z	20,113	5.4	4.5	3.8	3.2	2.6	2.2	1.8	1.4	1.1	0.9	0.7
25	I6	Pyroxenite		X	14,863	4.7	3.8	3.3	2.7	2.3	1.9	1.5	1.2	1.0	0.8	0.6
				Y	14,357	5.4	4.5	3.8	3.2	2.7	2.2	1.8	1.4	1.2	0.9	0.7
				Z	13,649	5.3	4.4	3.8	3.2	2.6	2.2	1.7	1.4	1.1	0.9	0.7
26	I7	Pyroxenite		X	14,121	14.9	12.8	11.0	9.4	7.9	6.6	5.4	4.4	3.6	2.9	2.3
				Y	12,375	13.9	12.0	10.4	8.8	7.5	6.2	5.2	4.2	3.5	2.8	2.2
				Z	15,738	12.3	10.5	9.1	7.7	6.5	5.4	4.5	3.7	3.0	2.4	1.9
27	I8	Pyroxenite		X	19,636	7.9	6.6	5.7	4.9	4.1	3.4	2.8	2.3	1.9	1.5	1.2
				Y	19,471	9.0	7.7	6.6	5.7	4.8	4.0	3.4	2.8	2.3	1.9	1.5
				Z	17,380	7.4	6.3	5.4	4.6	3.8	3.2	2.6	2.2	1.8	1.4	1.2
28	M10	Pyroxenite		X	14,862	20.5	17.9	15.7	13.6	11.6	9.8	8.2	6.8	5.6	4.6	3.7
				Y	18,231	21.5	18.8	16.5	14.3	12.2	10.4	8.7	7.2	6.0	4.9	4.0
				Z	23,566	17.2	14.9	13.0	11.1	9.4	7.9	6.6	5.4	4.5	3.6	2.9
29	E4	Serpentinite		X	1,112	16.2	12.5	9.6	7.2	5.2	3.8	2.7	1.9	1.3	0.8	0.5
				Y	930	23.0	18.2	14.4	11.1	8.5	6.4	4.8	3.6	2.6	1.9	1.4
				Z	768	18.4	14.1	10.8	8.0	5.8	4.0	2.7	1.8	1.1	0.6	0.3
30	M2	Serpentinite		X	29,443	12.4	10.5	8.9	7.5	6.3	5.2	4.3	3.5	2.8	2.3	1.8
31	M3	Serpentinite	Silicification	X	34,485	81.2	69.7	59.7	50.3	42.0	34.7	28.6	23.3	18.9	15.2	12.2
				Y	17,693	54.1	46.1	39.3	33.0	27.4	22.6	18.5	15.1	12.2	9.8	7.8
				Z	21,054	59.3	50.6	43.1	36.1	30.1	24.8	20.3	16.5	13.4	10.7	8.6
32	E3-5	Serpentinite	chromite	X	2,470	137.2	120.1	104.7	89.8	76.3	64.2	53.7	44.5	36.6	29.9	24.3
				Y	2,293	195.8	170.9	148.4	126.5	106.8	89.2	74.0	60.8	49.5	40.0	32.2
				Z	3,742	138.2	120.3	104.4	89.1	75.4	63.2	52.6	43.4	35.6	28.9	23.3
33	I1	Serpentinite		X	702	2.2	1.3	0.9	0.7	0.7	0.8	0.8	0.9	0.9	0.9	0.9
				Y	668	6.5	5.2	4.4	3.8	3.3	2.8	2.4	2.1	1.8	1.5	1.3
				Z	657	-6.2	-5.8	-5.0	-3.9	-2.9	-2.0	-1.3	-0.7	-0.3	0.1	0.3
34	I2	Serpentinite		X	5,188	20.1	17.0	14.5	12.1	10.0	8.3	6.8	5.5	4.4	3.5	2.8
				Y	6,792	17.3	14.6	12.5	10.5	8.7	7.2	5.9	4.8	3.8	3.1	2.4
				Z	5,057	17.1	14.4	12.2	10.2	8.5	7.0	5.7	4.6	3.7	3.0	2.4
35	I3	Serpentinite		X	32,445	30.1	25.7	22.0	18.5	15.5	12.8	10.6	8.6	7.0	5.6	4.5
				Y	27,492	34.8	29.8	25.6	21.6	18.1	15.0	12.4	10.1	8.2	6.7	5.3
				Z	30,145	30.7	26.2	22.5	18.9	15.8	13.1	10.8	8.8	7.2	5.8	4.6

Table II-3-6 Results of physical property tests (statistic)

ROCK TYPE	REM.	Resistivity(ohm-m)			chargeability(mV/V)		
		average	max	min	average	max	min
ALL SAMPLE		14,697	48,974	657	4.4	49.5	-0.3
Dolelite		45,020	48,974	41,799	0.7	0.8	0.6
Gabbro		7,275	10,941	4,885	4.9	7.3	3.4
Pyroxenite	Sulphide	15,398	27,634	3,462	1.8	2.5	1.0
Pyroxenite		16,456	39,328	4,570	2.8	6.0	0.7
Serpentinite		11,745	34,485	657	11.1	49.5	-0.3

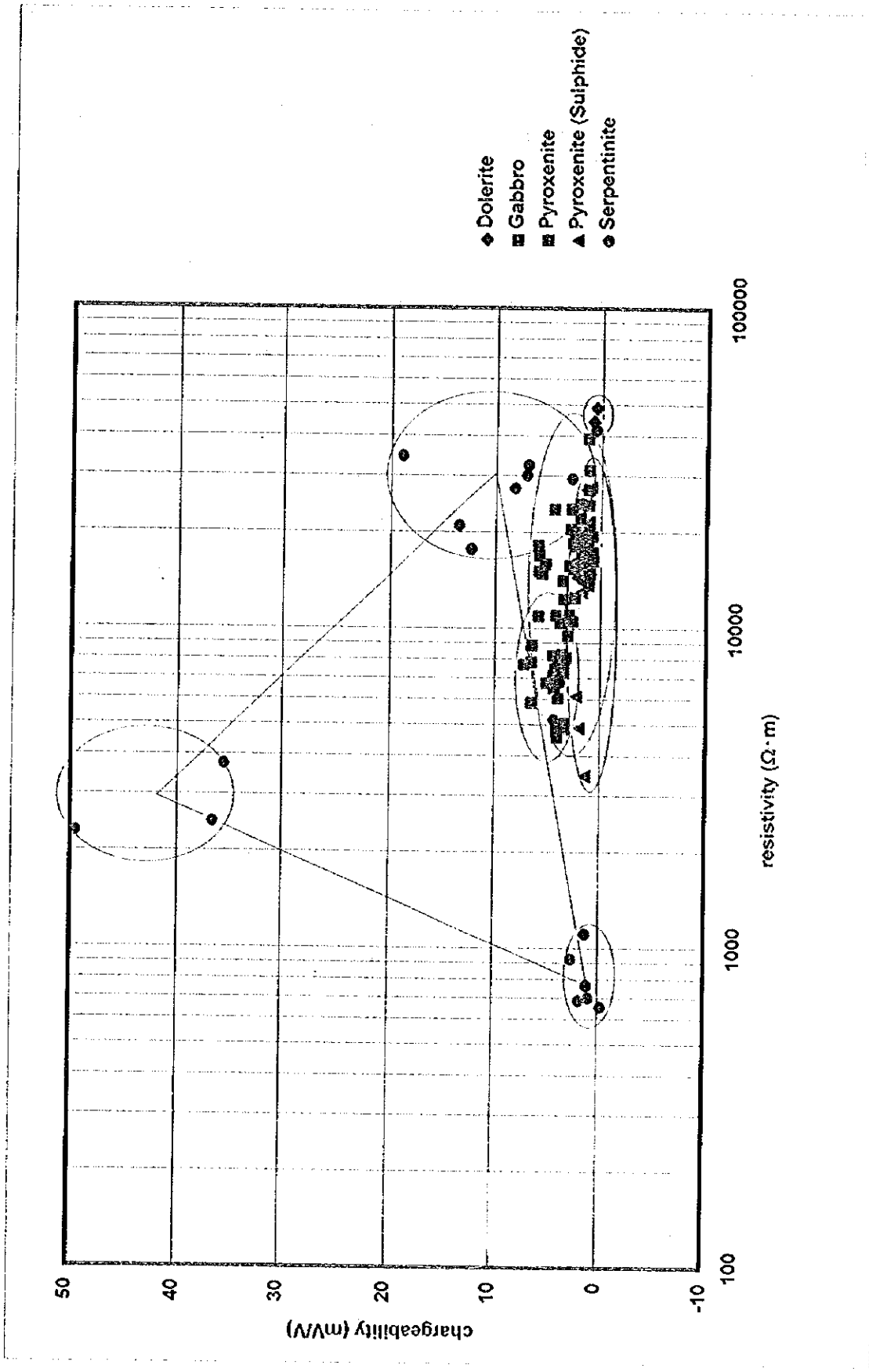

Fig.II-3-9 Relationship between chargeability and resistivity of rock and ore samples

chargeability.

Gabbro shows slightly higher chargeability (3.4 - 7.3mV/V) compare to other rocks and range in resistivity from 5,000 to 10,000 Ω·m.

Pyroxenite which has sulphide content shows low chargeability (2mV/V) and high resistivity (15,000 Ω·m). It is interpreted that the sulphide content is too low.

Serpentinite which has chromite($FeCr_2O_4$) content shows high chargeability(approximately 50mV/V). But Serpentinite which has no chromite content shows low chargeability. Serpentinite range in resistivity from 600 to 35,000 Ω·m. Serpentinite which shows high chargeability indicates high resistivity (2,000 - 3,000 Ω·m). Low resistivity of Serpentinite results from weathering.

3-5 Analysis of Geophysical Data

3-5-1 Method of 2-D Analysis

2-D simulation analysis of resistivity and chargeability pseudosection was carried out with finite element method forward program by Coggon(1971) and Rijo(1977). In these analyses, several ten times of repetition were made by forward mode of computation and amendment until the completion of approximation to pseudosection.

3-5-2 Results of 2-D Analysis

2-D simulation analysis was carried out for apparent resistivity/chargeability of provisional sections of 3 survey lines of E, I, L which were selected within deep chargeability anomalous zones. Data of physical properties of rocks and ore samples are used for this analyses as a reference. Geological sections of these 3 survey lines are shown in Fig.II-3-10.

The results of 2-D simulation analysis are shown in Fig.II-3-11 ~ Fig.II-3-13.

<Line E>

Resistivity: The low resistivity zone in the eastern part of station No.9 was generally matched with calculation by assuming the middle-resistivity body(200 ~ 500 Ω·m).

Chargeability: The chargeability anomalous pattern of the subsurface between stations No.4 and No.5 generally matched with calculation by assuming the polarizable body of 20 ~ 25mV/V in the surface area. The chargeability anomalous pattern at the deep part between stations No.8 and No.10 generally matched with calculation by assuming the small polarizable body (180 ~ 250 meters in depth, 100 meters in wide, 50 meters in thick, 120mV/V).

<Line I>

Resistivity: The low resistivity layer was estimated in the subsurface of the east part of station No.7. Gabbro predominate in this area.

Chargeability: The polarizable body of 25mV/V was estimated in the area of Serpentinite. The anomalous pattern of the deep part between stations No.6 and No.10 generally matched

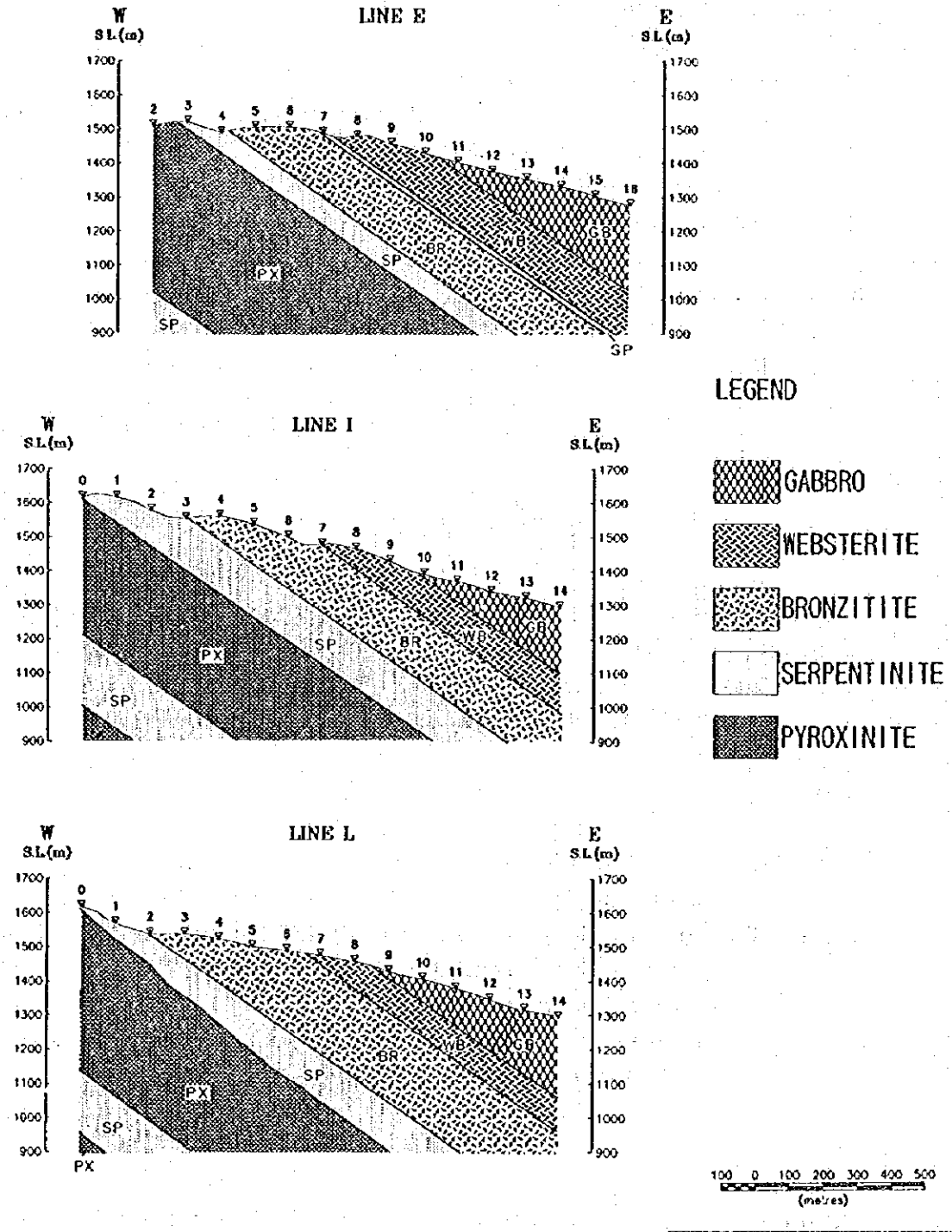

Fig.II-3-10 Geological sections on the geophysical survey lines

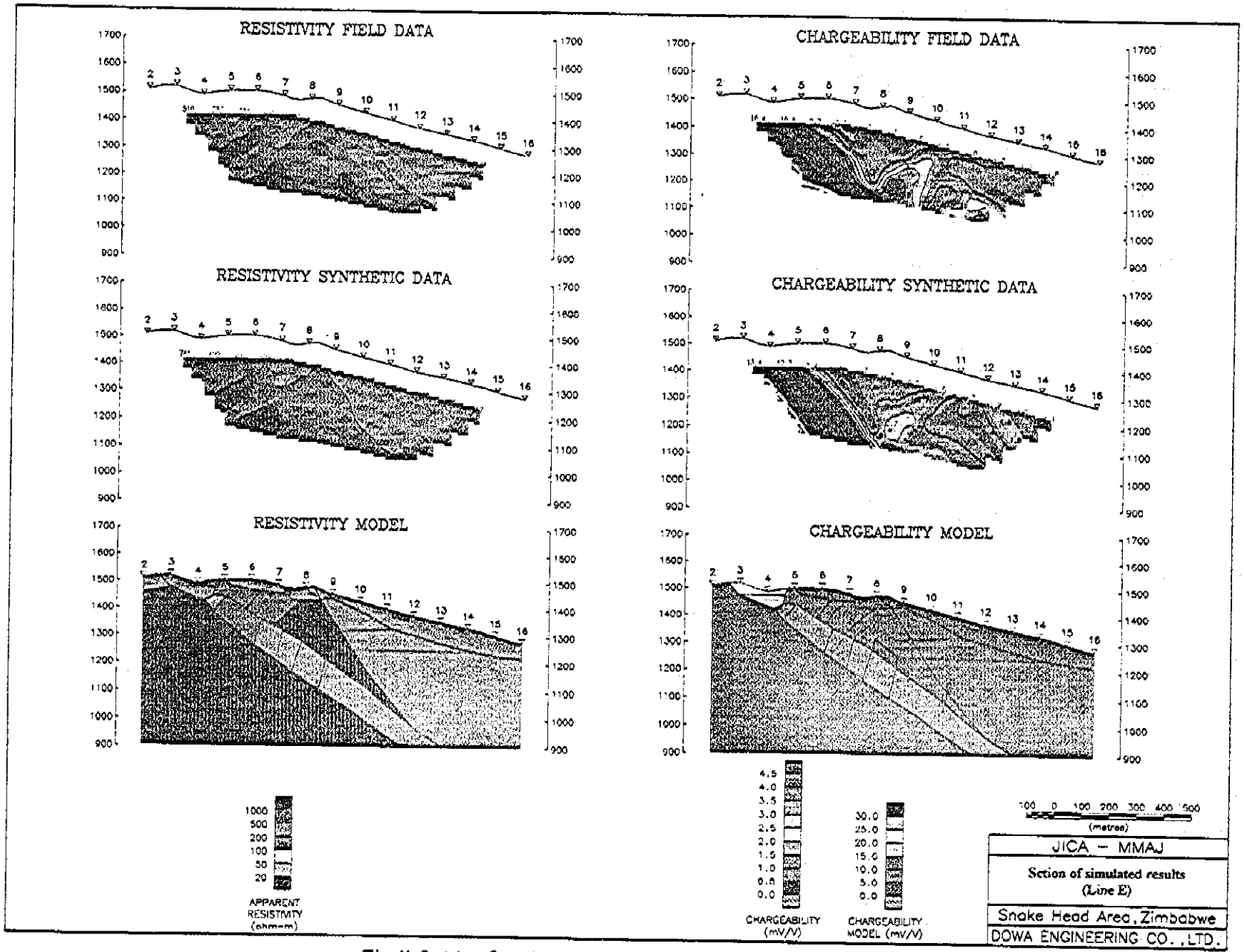

Fig.II-3-11 Section of simulated result (Line E)

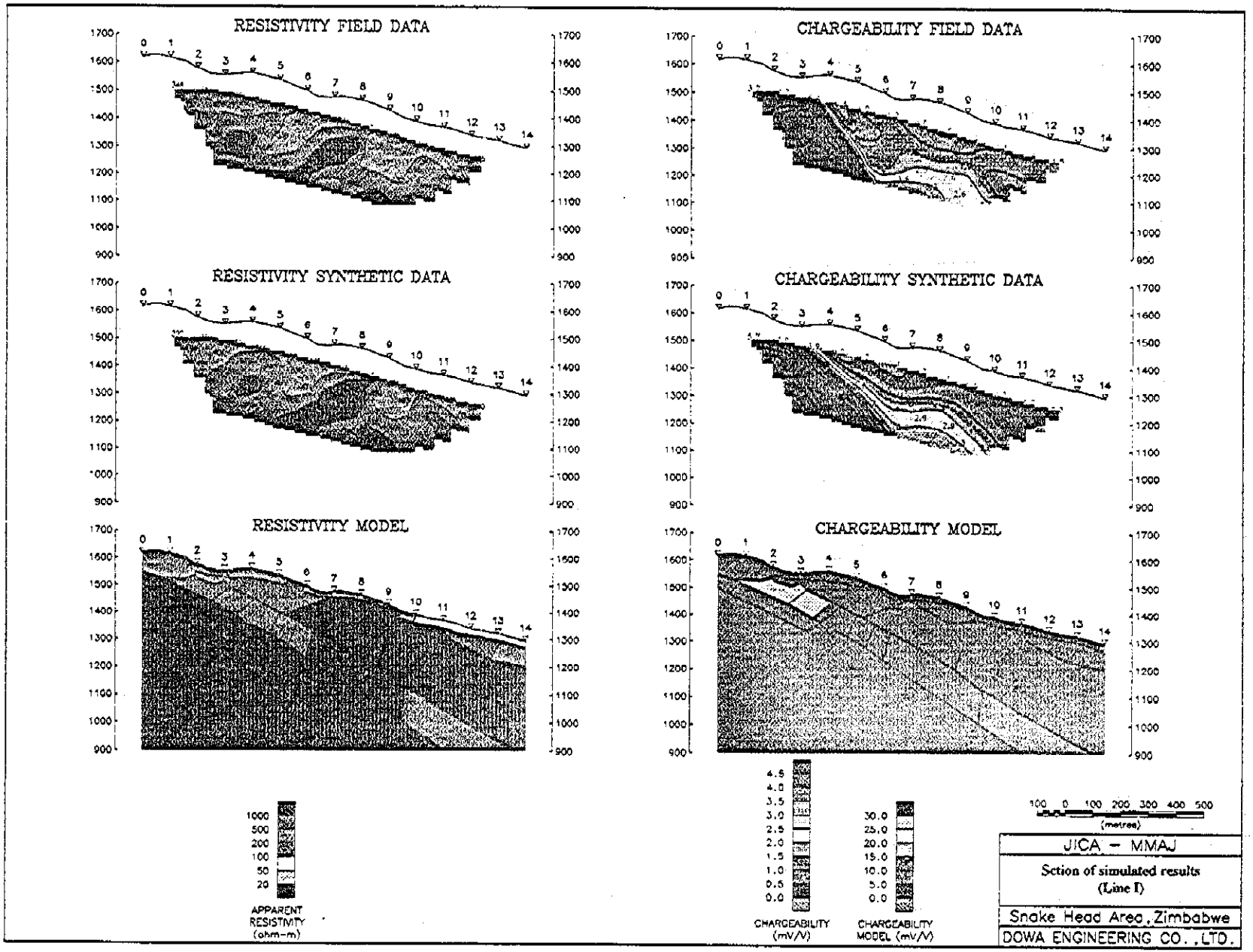

Fig.II-3-12 Section of simulated result (Line I)

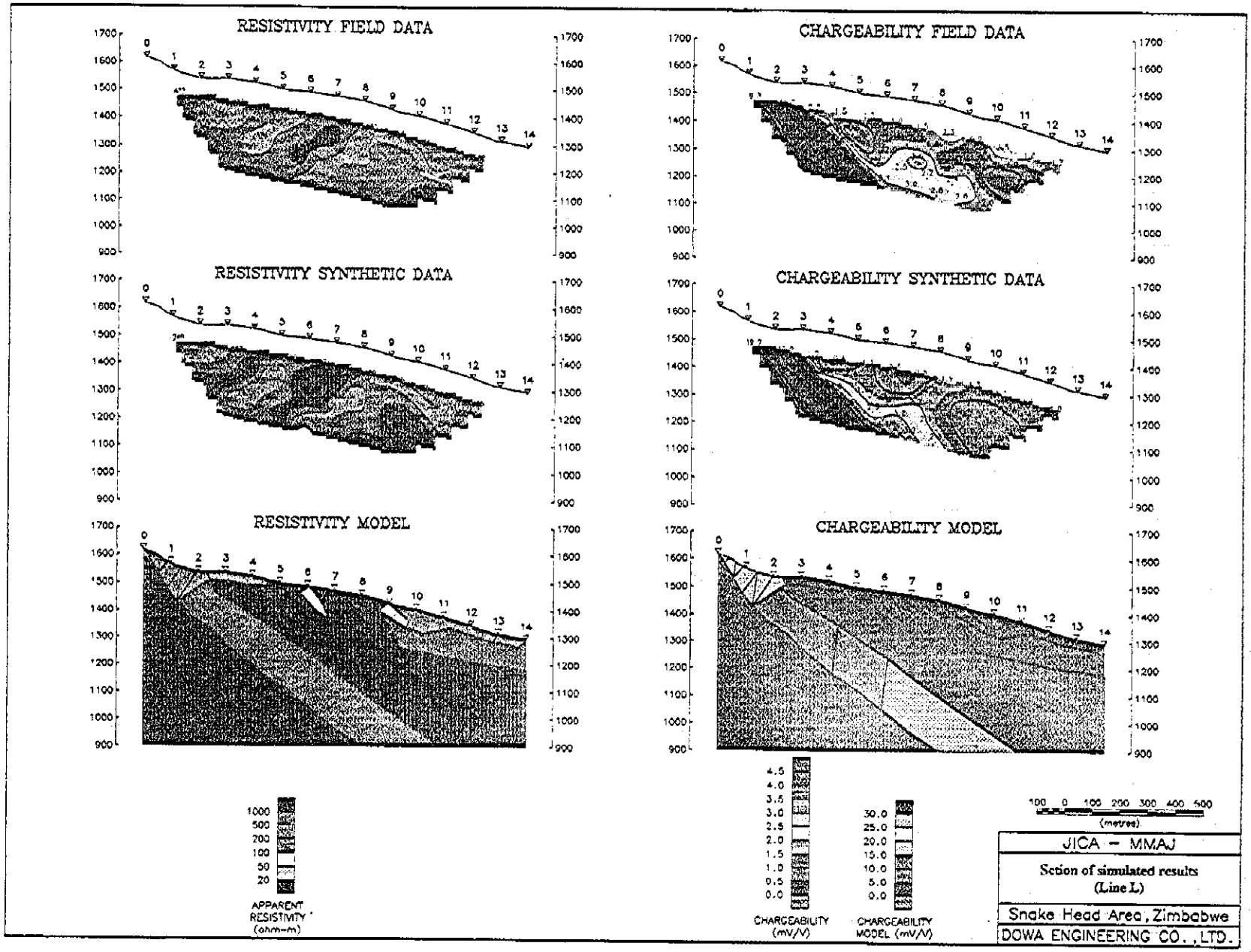

Fig.II-3-13 Section of simulated result (Line L)

with calculation by assuming the polarizable body of 30mV/V in the depth of approximately 170 meters. and approximately 100 meters thickness.

<Line I>

Resistivity: The low resistivity layer was estimated in the subsurface of the east of station No.9. Gabbro predominate in this area.

Chargeability: The polarizable body of 10 ~ 30mV/V was estimated in the subsurface between stations No.0 and No.2. The anomaly of the deep part between stations No.6 and No.7 generally matched with calculation by assuming the polarizable body(10 ~ 30mV/V, approximately 150 meters in thick) which is tilted to the east at an angle of 35 degree to the horizontal.

3-6 Evaluation of the Geophysical Survey

Results of comprehensive analysis of geophysical survey are shown in Fig II-3-14.

The distinctive chargeability anomalies were detected in the western part of Line D~P, and the weak distinctive anomalies were detected at deep part of Line E, and Line H~N between stations No.6 and No.10. These anomalies are not accompanied with low-resistivity anomalies.

As a result of physical property tests, it was proved that the sample which has sulphide content are in the order of 1.0mV/V to 2.5mV/V and do not show a great deal of contrast with the host rock. This probably results from minor quantities of sulphide. On the other hand, Serpentinite with chromite($FeCr_2O_4$) shows high chargeability(50mV/V), and also shows high resistivity(over 500 Ω·m). Difference was found between this sample and other rocks in chargeability.

As a result of 2-D simulation analysis, it was estimated that the anomaly in the western part of area result from polarizable body which correspond to Serpentinite. And it was also estimated that the anomaly at the deep part between stations No.6 and No.10 result from polarizable body which correspond to the extension of Serpentinite or the basal part of Pyroxenite(P1).

According to EPO654(1992), drilling has succeeded in finding the two zones of disseminated sulphide mineralization. These zones are termed the main sulphide zone(MSZ; 85 ~ 95 meters in depth) and the lower sulphide zone(LSZ; 145 ~ 155 meters in depth), and it has been made clear that the two zones are 10m thick and contain 0.1 ~ 0.12 % Cu + Ni.

On the basis of above results, it can be stated that the anomalies at shallow part in western part of Line D ~ Line P result from Serpentinite with chromite. On the other hand, It can be stated that the anomalies at deep part of Line E and Line H ~ N between stations No.6 and No.10 result from the extension of Serpentinite or the basal part of Pyroxenite(P1). It may be inferred that the source of these anomalies are situated approximately 150 meters below LSZ.

The relationship between grade of sulphide and chargeability can not be decided because of the variety of resistivity of host rock or connection between each sulphide minerals. But it can be stated that it is difficult to find out low-grade sulphide target(under %-order) by IP survey.

Data from 2-D simulation analysis and physical property tests, as well as field data, indicate that the boundary between Pyroxenite(P1) and Serpentinite has been made clear.

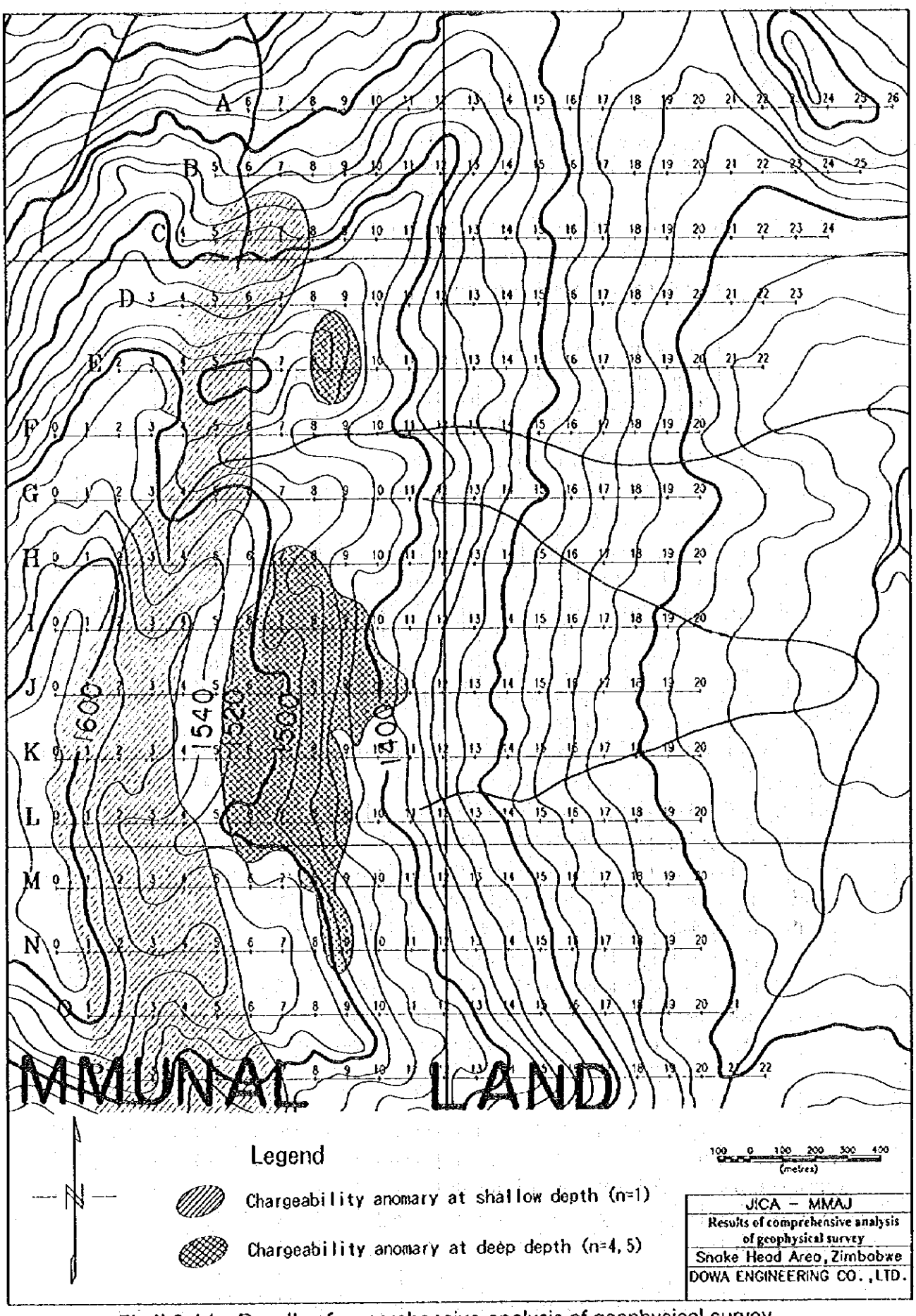

Fig.II-3-14 Results of comprehensive analysis of geophysical survey

Chapter 4 Considerations of the Survey Results

4-1 Controls on Mineralization Related to the Geological Structure and Characteristics of the Mineralization

The Great Dyke is a layered basic intrusion, whose PGM, Ni, and Co ore deposits are reported to occur mainly in the P1 layer just under the gabbroic rocks.

Same mineralized zone was recognized in the Mimosa Mining area of Wedza complex, The Unki area of the Selukwe complex, and the Zinka, Selous, Hartley mining area of the Hartley complex.

Upper gabbroic rocks are widely distribute in the center portion of the survey area. Rock facies move to lower peridotite(dunite, harzburgite) pass through multi layered pyroxenite.

The sulphide mineralization which can be observed with naked eye mainly occur in the P1 layer of the upper most pyroxenite layer. Chromite occur mainly in the lower pyroxenite layer.

Sulphide minerals in the mineralized zone consist of pyrrhotite, pentlandite, chalcopyrite as essential minerals and the pyrite, magnetite, chromite as a accessory minerals. Small quantities of violarite, millerite, goethite occurring as secondary minerals were also recognized.

Layering in the western block shows a N-S to NE-SW direction of strike and E to SE direction of dip, whereas the layering in the central block shows a N-S direction of strike and E direction of dip in the northern portion and W direction of dip in the southern portion. The layering in the eastern block shows a N-S to NE-SW direction of strike and W to NW direction of dip.

These layering can be pursued in the field.

4-2 Relationship between Geochemical Anomaly and the Mineralization

(1) Metal concentration and geological position

Gold, platinum, and palladium show a narrow continuous distribution, confined to the middle portion of the P1 layer. Platinum and palladium were also partially detected in the serpentinite layer, below P1 pyroxenite.

Silver and rhodium show low grade and wide a distribution, not corresponding to geology. Silver has no correlation with other elements, suggesting that it has a different condition of concentration compared to these elements. Distribution of the population of Rhodium is difficult because samples shown above the detectable limit are very few.

Copper is divided into 2 clear different populations, continuously concentrated in upper portion of P1 layer. Sulphide dissemination which correspond to high copper concentrated zone is recognized in the field, therefore, copper concentrated zone suggest to existence of mineralization.

Cobalt and nickel show a clear and continuous zone high concentration in the lower portion of P1 layer and lower serpentinite layer. The distribution of cobalt and nickel seem to reflect the geology.

Gold-platinum-palladium group, copper, and cobalt-nickel group have no clear correlation each other, and have different distributions in the field. These groups seem to have no related mineralization.

(2) Comparison of each geochemical survey area

As regard gold and PGM elements, the area expected to high concentration of metals is the WS area, followed by the northeastern portion of the WN area and northern portion of CB area. though the

southwestern portion of the WN area is divided into small area by faulting, local metal concentration are recognized. Southern portion of the CB area shows weak metal concentrations, distribution of concentrations become patchy. EN and ES areas show no concentration.

4-3 Relationship between Geophysical Anomaly and the Mineralization

The characteristics of high chargeability anomalies in this area is not accompanied by low resistivity distribution.

As a result of physical property tests, it was proved that the sample which has sulphide content are in the order of 1.0mV/V to 2.5mV/V and do not show a great deal of contrast with the host rock. This probably results from minor quantities of sulphide. On the other hand, Serpentinite with chromite($FeCr_2O_4$) shows high chargeability(50mV/V), and also shows high resistivity(over 500 W×m). Difference was found between this sample and other rocks in chargeability.

As a result of 2-D simulation analysis, it was estimated that the anomaly in the western part of area result from polarizable body which correspond to Serpentinite. And it was also estimated that the anomaly at the deep part between stations No.6 and No.10 on E, H, I, J, K, L, M, N survey lines result from polarizable body which correspond to the deeper part of Serpentinite or the basal part of Pyroxenite(P1).

The relationship between grade of sulphide and chargeability can not be decided because of the variety of resistivity of host rock or connection between each sulphide minerals. But it can be stated that it is difficult to find out low-grade sulphide target(under %-order) by IP survey.

4-4 Potentialities of Expected Ore Deposits

Expected ore deposits in this area are stratabound PGM, nickel, cobalt, and copper ore deposits.

As the result of the geological survey, the P1 layer which is thought to host ore deposits was investigated in the field. It was identified that the P1 layer occurs under the gabbroic rocks in the central and north eastern portion of the survey area. Sulphide dissemination was recognized in upper portion of the P1 layer, suggesting the existence of the mineralization.

Geochemical survey indicated that gold and PGM elements are concentrated in the WS area, followed by northeastern portion of the WN area and northern portion of CB area.

Geophysical surveys identified chargeability anomalies deep below No.6 to 10 stations on E, H, I, J, K, L, M, N survey lines suggesting existence of a chargeable body at the bottom of the P1 layer, or extension of serpentinite layer.

Based on the above facts, WS area, northeastern portion of the WN area and northern portion of CB area in this survey area are considered to have high potential for occurrence of new ore deposits similar to the Mimosa mine in the Wedza complex, the Unki area in the Selukwe complex, and the Zinka, Selous, Hattley mine in the Hartley complex.

Part III Conclusion and Recommendation

Part III Conclusion and Recommendation
Chapter 1 Conclusion

The literature search(150km^2), the geological survey and the geochemical survey(22.25km^2), and geophysical survey(total line length 32km) were carried out in this fiscal year as the Phase I of this project.

The literature search :

There are publications of the GSD such as the Geologic Maps, Geological Survey Bulletin of Zimbabwe and E.P.O.s' reports. The compiled geological map was made based on these data.

Geology of this area consists of gneiss and granites of Archaean era which forms the basement, and ultramafic to mafic rocks of the Great Dyke which intruded in to the basement rocks.

PGM is mainly in the upper most layer(P1) of multi layered pyroxenite, and chromite occur in the lower pyroxenite layers.

In the Snake Head area Union Carbide and Cluff carried out a geological survey and exploration.

In the Snake Head area continuous distribution of pyroxenite P1 just under the gabbroic rock was recognized same to known platinum mining area, and Union carbide and Cluff obtained some platinum showing by their drilling, therefore, it is considered to have high potentiality of occurrence of new ore deposits.

Geochemical surveys :

PGM minerals are closely related to the sulfide minerals like the pyrite, pyrrhotite, chalcopyrite and petlandite, etc., and accompanied with marginal zone of sulphide(E.P.O.654).

The sulphide mineralization which can observe with naked eye continuously occur in the upper portion of the P1 layer in the WS area.

As the result of the microscopic observation of ore polish sections, sulphide mineralization zone in this area generally consist of pyrrhotite, pentrandite, chalcopyriye, Pyrite, magnetite and chromite.

The areas of potentialities of PGM ore deposit occurrences are considered to be the distribution area of the P1 layer.

Geochemical survey areas were determined based on the results of the existing data analysis and geological survey on the distribution area of the P1 layer.

The numbers of the analyzed elements are 8. They are Au, Ag, Cu, Co, Ni, Pt, Pd and Rh.

Gold, platinum, and palladium show a narrow continuous distribution, confined to the middle portion of the P1 layer. Platinum and palladium were also partially detected in the serpentinite layer, below P1 pyroxenite.

Copper is divided into 2 clear different populations, continuously concentrated in upper portion of P1 layer. Sulphide dissemination which correspond to high copper concentrated zone is recognized in the field, therefore, copper concentrated zone suggest to existence of mineralization.

Cobalt and nickel show a clear and continuous zone high concentration in the lower portion of P1 layer and lower serpentinite layer. The distribution of cobalt and nickel seem to reflect the geology.

As regard gold and PGM elements, the area expected to high concentration of metals is the WS

area, followed by the northeastern portion of the WN area and northern portion of CB area.

Geophysical surveys :

The distinctive chargeability anomalies were detected in the western part of Line D~P, and the weak distinctive anomalies were detected at deep part of Line E, and Line H~N between stations No.6 and No.10. These anomalies are not accompanied with low-resistivity anomalies.

As a result of 2-D simulation analysis, it was estimated that the anomaly in the western part of area result from polarizable body which correspond to Serpentinite. And it was also estimated that the anomaly at the deep part between stations No.6 and No.10 result from polarizable body which correspond to the deeper part of Serpentinite or the basal part of Pyroxenite(P1).

On the basis of above results, it can be stated that the anomalies at shallow part in western part of Line C ~ Line P result from Serpentinite with chromite. On the other hand, It can be stated that the anomalies at deep part of Line E and Line H ~ N between stations No.6 and No.10 result from the deeper part of Serpentinite or the basal part of Pyroxenite(P1).

The relationship between grade of sulphide and chargeability can not be decided because of the variety of resistivity of host rock or connection between each sulphide minerals. But it can be stated that it is difficult to find out low-grade sulphide target(under %-order) by IP survey.

Data from 2-D simulation analysis and physical property tests, as well as field data, indicate that the boundary between Pyroxenite(P1) and Serpentinite has been made clear.

summary :

Expected ore deposits in this area are stratabound PGM nickel, cobalt, and copper ore deposits.

P1 layer which is thought to host ore deposits was geologically investigated in the field, and it was identified that the P1 layer occurs under the gabbroic rocks in the central and north eastern portion of the survey area. Sulphide dissemination was recognized upper potions of the P1 layer, suggesting existence of the mineralization.

Result of the geochemical survey indicate that gold and PGM element concentrations are expected in the WS area, followed by the northeastern portion of the WN area and northern portion of CB area.

Result of the geophysical surveys identified chargeability anomalies deep below No.6 to 10 stations on E, H, I, J, K, L, M, N survey lines suggesting existence of chargeable body in bottom of the P1 layer or extension of serpentinite layer below P1.

Based on the above facts, WS area, northeastern portion of the WN area and northern portion of CB area in this survey area is considered to have high potential for occurrence of new ore deposits similar to the Mimosa mine in the Wedza complex, the Unki area in the Selukwe complex, and the Zinka, Selous, Hattley mine in the Hartley complex.

Chapter 2 Recommendation for the Phase II

Based on the survey results of the Phase I, the method of the survey for the phase II are proposed as follows :

1. The detailed geological and geochemical survey

Detailed geological, and geochemical surveys be carried out in portion of WS area, north-eastern portion of the WN and northern portion of CB. The survey should include closely spaced rock sampling and trenching across P1 locate the mineralized horizon.

2. The geophysical survey

Geophysical survey should be carried out in areas of geochemical anomalies in the north-eastern portion of the WN area and northern portion of CB area to investigate the possibility of sulphide horizon.

3. Drillings

Drilling in the most anomalous areas outlined in Phase I survey must be carried out in order to investigate the possibilities of the existence of Au and PGM mineralization.